Title

Direct involvement of Hsp70 ATP hydrolysis in Ubr1-dependent quality control.

Journal

Molecular biology of the cell, 31(24)

ISSN

1059-1524

Authors

Singh, Amanjot
Vashistha, Nidhi
Heck, Jarrod
et al.

Publication Date

2020-11-01

DOI

10.1091/mbc.e20-08-0541

Peer reviewed

Direct involvement of Hsp70 ATP hydrolysis in Ubr1-dependent quality control

Amanjot Singh[a,†,*], Nidhi Vashistha[a], Jarrod Heck[b], Xin Tang[a], Peter Wipf[c], Jeffrey L. Brodsky[d], and Randolph Y. Hampton[a,*]

[a]Division of Biological Sciences, University of California, San Diego, La Jolla, CA 92103; [b]Adaptive Biotechnologies Corp., Seattle, WA 98102; [c]Department of Chemistry and [d]Department of Biological Sciences, University of Pittsburgh, Pittsburgh, PA 15260

ABSTRACT **Chaperones can mediate both protein folding and degradation. This process is referred to as protein triage, which demands study to reveal mechanisms of quality control for both basic scientific and translational purposes. In yeast, many misfolded proteins undergo chaperone-dependent ubiquitination by the action of the E3 ligases Ubr1 and San1, allowing detailed study of protein triage. In cells, both HSP70 and HSP90 mediated substrate ubiquitination, and the canonical ATP cycle was required for HSP70's role: we have found that ATP hydrolysis by HSP70, the nucleotide exchange activity of Sse1, and the action of J-proteins are all needed for Ubr1-mediated quality control. To discern whether chaperones were directly involved in Ubr1-mediated ubiquitination, we developed a bead-based assay with covalently immobilized but releasable misfolded protein to obviate possible chaperone effects on substrate physical state or transport. In this in vitro assay, only HSP70 was required, along with its ATPase cycle and relevant cochaperones, for Ubr1-mediated ubiquitination. The requirement for the HSP70 ATP cycle in ubiquitination suggests a possible model of triage in which efficiently folded proteins are spared, while slow-folding or nonfolding proteins are iteratively tagged with ubiquitin for subsequent degradation.**

Monitoring Editor
James A. Olzmann
University of California, Berkeley

Received: Sep 3, 2020
Accepted: Sep 18, 2020

INTRODUCTION

The ubiquitin proteasome system (UPS) is responsible for the destruction of numerous proteins in eukaryotes (Zattas and Hochstrasser, 2015; Hampton and Dargemont, 2017; Pohl and Dikic, 2019). In its simplest form, ubiquitin-mediated destruction of proteins occurs by covalent modification of a targeted substrate with one or more multiubiquitin chains, which allow recognition and subsequent proteolysis of the ubiquitinated protein by the 26S proteasome. Accordingly, the selection of proteins for ubiquitination is the underlying feature that allows for the high specificity of degradation that hallmarks this pathway. Proteins undergo ubiquitination by the sequential action of three classes of enzymes: an ATP-dependent E1 ubiquitin-activating enzyme (UBA), which transfers a chemically active form of ubiquitin to E2 ubiquitin-conjugating enzymes (UBC), from which an E3 ubiquitin ligase brokers the transfer of the UBC-bound ubiquitin to the substrate or to the growing multiubiquitin chain (Wangeline *et al.*, 2017). Understanding the action of the large and expanding list of ubiquitin E3s lies at the heart of specificity and target selection in the UPS pathway.

Protein quality control (QC) maintains misfolded proteins at acceptable levels. Such mechanisms exist in all domains of life and are important in limiting lethal proteotoxic stresses that arise from misfolded proteins. The two main actions of the various QC pathways are to refold misfolded proteins by the action of chaperones, or to lower the effective concentration through sequestration or degradation. Aberrations in protein QC have been implicated in a number of

This article was published online ahead of print in MBoC in Press (http://www.molbiolcell.org/cgi/doi/10.1091/mbc.E20-08-0541) on September 23, 2020.

Author contributions: A.S. and R.Y.H. conceived and curated the project; A.S. was the central experimentalist in the day-to-day line of inquiry. N.V., J.H. and X.T. performed important individual experiments included in the work. J.L.B. and P. W. provided reagents, planned experiments, and helped in analysis. N.V. created the model in Figure 7.

†Present address: National Centre for Biological Sciences, Tata Institute of Fundamental Research, Bengaluru 560064, India.

*Address correspondence to: Randolph Y. Hampton (rhampton@ucsd.edu) or Amanjot Singh (amanjot.singh@gmail.com).

Abbreviations used: CHX, cycloheximide; co-IP, coimmunoprecipitation; CPY, carboxypeptidase Y; CQC, cytoplasmic protein quality control; DMSO, dimethyl sulfoxide; ERAD, endoplasmic reticulum–associated degradation; GND1, 6-phosphogluconate dehydrogenase; IgG, immunoglobulin G; NEF, nucleotide exchange factor; QC, quality control; RAD, radicicol; WT, wild type.

human maladies and the aging processes that affect all tissues (Balch *et al*., 2008; Guerriero and Brodsky, 2012; Klaips *et al*., 2018; Hipp *et al*., 2019; Rosenzweig *et al*., 2019). In eukaryotes, one branch of protein QC systems recognizes and destroys misfolded proteins by the UPS pathway. The study of this widely used pathway for protein destruction has revealed QC E3 ligases that mediate the ubiquitination of a subset of misfolded substrates. Examples include endoplasmic reticulum–associated degradation (ERAD), nuclear QC, ribosome-associated QC, inner nuclear membrane QC, and cytoplasmic QC (Hampton and Sommer, 2012; Lykke-Andersen and Bennett, 2014; Brandman and Hegde, 2016; Enam *et al*., 2018; Joazeiro, 2019; Phillips *et al*., 2020). In each case, a wide range of misfolded or misassembled substrates are recognized, usually by one or a few E3s to bring about selective ubiquitination and subsequent destruction. How a single QC E3 specifically recognizes such a large group of potential misfolded substrates remains an important and pressing question.

QC E3 ligases appear to utilize two main mechanisms to accomplish a broad-yet-selective recognition of misfolded substrates. Some QC ligases employ chaperones to detect and degrade misfolded substrates. For example, mammalian carboxy terminus of Hsc70 interacting protein (CHIP) forms a complex with HSP70 chaperones to facilitate ubiquitination, which is executed by the U box of the CHIP protein (Qian *et al*., 2006). Similarly, Hrd1 employs the ER lumenal HSP70 Kar2 (BiP in mammals) and associated HSP40 cochaperones to assist in recognition of lumenal misfolded substrates (Nishikawa *et al*., 2001). Alternatively, some E3s appear to autonomously recognize misfolded proteins by virtue of sequence and structural features. Both the nuclear E3 San1 and the ERAD ligase Hrd1 can directly detect QC substrates without the help of ancillary folding factors (Gardner *et al*., 2005; Sato *et al*., 2009; Rosenbaum *et al*., 2011; Wu *et al*., 2020). These properties are not mutually exclusive; for example, Hrd1 detects integral membrane ERAD substrates (ERAD-M) autonomously but employs lumenal HSP70 Kar2 to efficiently degrade soluble, lumenal ERAD substrates (ERAD-L).

Chaperone-dependent ubiquitination has been observed in a variety of circumstances (McClellan *et al*., 2005; Park *et al*., 2007; Heck *et al*., 2010; Kriegenburg *et al*., 2014; Kandasamy and Andreasson, 2018). A study of this form of degradative QC raises several important and challenging questions of both basic and medical interest. First, since chaperones also participate in refolding damaged proteins, it is unclear how the decision to ubiquitinate rather than to refold is made. Second, to what extent are the mechanisms that govern chaperone action at play in ubiquitin-mediated degradation? For example, is the classic nucleotide-dependent cycle of capture-and-release employed in substrate degradation? Third, which chaperone families and which accompanying cochaperones operate during the course of these degradative pathways? And finally, how do chaperones trigger ubiquitination of misfolded substrates? A variety of roles for chaperones can be envisioned, including direct participation in substrate recognition (as appears to be the case with CHIP), assisting in substrate transport into a compartment where degradation occurs, or alteration of a substrate's accessibility by changing the physical state of a misfolded substrate to facilitate E3 interaction. Again, these mechanisms need not be mutually exclusive.

We have been addressing these questions through studies of cytoplasmic protein quality control (CQC; Heck *et al*., 2010). In yeast, a variety of mutant, truncated, and full-length misfolded proteins undergo degradation by the action of two E3 ligases, Ubr1 and San1, that appear to operate in parallel (Heck *et al*., 2010; Khosrow-Khavar *et al*., 2012; Metzger *et al*., 2020; depicted in Figure 1A). We and others have observed that both of these degradative pathways require cytoplasmic HSP70 in vivo (Heck *et al*., 2010; Nillegoda *et al*., 2010; Prasad *et al*., 2010). Furthermore, the HSP110 cochaperone, Sse1, is critical for substrate ubiquitination mediated by either E3. This broad requirement for HSP70 occurs in a fairly complex cellular environment. Our work indicates that Ubr1 functions in the cytosol, while San1 encounters substrates in the nucleus (Heck *et al*., 2010). Furthermore, San1 functions in misfolded protein recognition in an autonomous manner, by virtue of a natively unstructured region that recognizes exposed hydrophobic motifs in misfolded proteins (Rosenbaum *et al*., 2011). We and others have found that the entry of a model substrate into the nucleus is chaperone-dependent; therefore, the San1 dependence may arise from substrate delivery (Heck *et al*., 2010; Prasad *et al*., 2010, 2018). Furthermore, misfolded substrates may either be soluble or form large deposits (Doyle *et al*., 2013), which can obscure the definition of the actual role(s) of chaperones in protein degradation. More recently, it has been shown that proteins in the cytoplasm and nucleus are ubiquitinated differently; while in the cytoplasm, both lysine 48 (K48)- and lysine 11 (K11)-linked ubiquitin chains are important for UPS-mediated degradation, but in the nucleus, the degradation of misfolded proteins requires only K48-linked chains (Samant *et al*., 2018).

In this work, we have directly addressed the role of chaperones in Ubr1-mediated CQC by employing a variety of substrates (Figure 1A). We have found that both HSP70 and HSP90 are critically important for degradation of all the substrates that we tested in vivo. Furthermore, the HSP70 ATP hydrolysis cycle—as well as the cochaperones that modify cycle dynamics—are required for substrate ubiquitination. By developing an immobilized substrate, in vitro assay that precludes possible effects on the physical state of the substrate, such as compartmentalization, aggregation, or solubilization, we have been able to examine in better detail how chaperone action functions in Ubr1-dependent client selection and ubiquitin tagging. In that assay, HSP70 was directly involved with Ubr1-mediated substrate ubiquitination, while HSP90 played only a significant and general role in the intact cell. In the HSP70-dependent direct actions revealed in vitro, the ATPase cycle was also required for Ubr1-mediated QC. These findings suggest a kinetic model for chaperone-mediated triage, in which efficiently folded proteins are spared from degradation, while poorly folding or nonfolding proteins are ubiquitinated and degraded.

RESULTS

Both HSP90 and HSP70 were required for cytoplasmic QC

In our initial studies, we found that the primary HSP70 chaperone in yeast, Ssa1, was required for the degradation of CQC substrates (Heck *et al*., 2010; Figure 1B). Cells lacking both Ssa1 and Ssa2 exhibited strong stabilization of both Ubr1/San1 substrates Δss-CPY*-GFP and tGnd1-GFP (Figure 1B).

San1 can work independently of chaperones in the recognition and ubiquitination of some substrates (Rosenbaum *et al*., 2011; Guerriero *et al*., 2013). We previously posited that the chaperone requirement of the San1-dependent branch of cytoplasmic QC was due to the requirement for nuclear import, where San1 resides (Heck *et al*., 2010). Accordingly, we tested the role of HSP70 during the degradation of an exclusively Ubr1-dependent misfolded substrate, stGnd1 (Heck *et al*., 2010). This substrate similarly showed strong dependence on HSP70 during Ubr1-mediated degradation (Figure 1B). These and other data all point to a universal role of HSP70 in the degradation of cytoplasmic substrates, although perhaps through a number of independent mechanisms (Gowda *et al*., 2013; Guerriero *et al*., 2013; Gallagher *et al*., 2014; Kandasamy and Andreasson, 2018).

We also tested the role of HSP90 chaperones in degradation of cytoplasmic substrates by genetic and pharmacological means. To this end, we employed a strain in which both native loci of the cytoplasmic HSP90 genes were null (*hsp82*Δ*hsc82*Δ), with the essential HSP90 activity provided by either a wild-type (WT) (*HSP82*) or ts (*hsp82*G170D) allele (Nathan and Lindquist, 1995). These strains showed clear stabilization of both Ubr1/San1 substrates, as well as the Ubr1-specific stGnd1 substrate (Figure 1C). We also discovered that two HSP90 inhibitors, radicicol (RAD) and geldanamycin, slowed the degradation of both Ubr1/San1 substrates, as well as the Ubr1-specific substrate stGnd1 (Figure 1D; effects of RAD are shown). This Hsp90 dependence has also been seen in earlier studies on degradation of misfolded VHL (McClellan *et al.*, 2005).

Ubiquitin-mediated degradation is a multi-step process that can require factors before, during, and/or after covalent addition of multiubiquitin chains (Lee *et al.*, 2011). We previously showed that HSP70 was required for in vivo ubiquitination of cytoplasmic substrates (Heck *et al.*, 2010). We similarly tested the role of HSP90 in this process and found that, like HSP70, the ubiquitination of several substrates was affected in vivo by either the stabilizing alleles or drugs that cause stabilization (Figure 1E; Supplemental Figure 1).

Sse1 (HSP110) was required for CQC

On the basis of the above data, we next utilized a variety of in vivo and in vitro approaches to understand the role(s) of unique chaperones during the degradation of misfolded proteins. In our prior work, the two strongest effects on the degradation of cytoplasmic misfolded proteins were observed with the *sse1*Δ null and the *ydj1*Δ null strains (Heck *et al.*, 2010). The loss of Sse1 has a particularly strong effect, causing nearly complete stabilization of the substrates tested. The role of this cochaperone is particularly interesting in light of the requirements for both HSP70 and HSP90, since Sse1 is known to function with each of these central chaperones, although in different ways: acting directly as a nucleotide exchange factor (NEF) for HSP70 (Dragovic *et al.*, 2006; Raviol *et al.*, 2006; Shaner *et al.*, 2006) and indirectly with HSP90 via a HSP70–HSP90 complex (Liu *et al.*, 1999; McClellan *et al.*, 2005). Sse1, also known as HSP110, is a homologue of HSP70 with the capacity to bind unfolded substrates and hydrolyze ATP. However, it is best understood as a NEF for HSP70, catalyzing the exchange of ADP for ATP and triggering the transition from the high- to the low-affinity peptide-binding state (Dragovic *et al.*, 2006; Raviol *et al.*, 2006; Goeckeler *et al.*, 2008). We therefore tested which function(s) of Sse1 were required for its broad role in the degradation of misfolded cytoplasmic proteins. We queried the importance of Sse1 for NEF activity by complementing a *sse1*Δ null mutant with either WT Sse1 or the mutants $Sse1^{K69Q}$, a point mutant that cannot hydrolyze ATP, and $Sse1^{G233D}$, a point mutant that cannot bind ATP (Shaner *et al.*, 2005, 2006) (Figure 2A). $Sse1^{G233D}$ deficient for NEF activity stabilized the tested substrates, indicating the contribution of this activity in degradation. Importantly, the Ubr1-specific substrate stGnd1 was stabilized, as were substrates like Δss-CPY*-GFP and tGnd1-GFP that employ both Ubr1 and San1. Therefore, the ability of Sse1 to effect nucleotide exchange on HSP70 has a broad role in degrading misfolded proteins that originate in the cytosol.

HSP70 ATP hydrolysis was required for CQC degradation

The requirement for nucleotide exchange involving Sse1 suggested that ATP hydrolysis by HSP70 was required for CQC. Because removal of all HSP70 activity is lethal, we employed the double null *ssa1*Δ*ssa2*Δ strain, with deletions of two of the four cytoplasmic HSP70 *SSA* genes, to examine the role of cytoplasmic HSP70 function in CQC. The *ssa1*Δ*ssa2*Δ strain is viable but shows strong decrement in the degradation of a variety of CQC substrates in vivo (Figure 1B; Heck *et al.*, 2010; Prasad *et al.*, 2010). Accordingly, this strain can be used as a background for plasmid-based expression of HSP70 mutants to evaluate their abilities to restore CQC. *ssa1*Δ*ssa2*Δ strains were constructed to express WT HSP70-encoding *SSA1* or various mutants to examine the importance of ATP binding and hydrolysis. Degradation of the San1/Ubr1-dependent substrates tGND1-GFP or the exclusively Ubr1-dependent substrate stGND1 was restored by the WT protein but not by the mutants, which are unable to hydrolyze ($Ssa1^{K69Q}$) or bind ($Ssa1^{G198D}$) ATP (Figure 2B; McClellan and Brodsky, 2000). This result indicated that the ATP hydrolytic cycle of HSP70 was required for degradation of these substrates.

Diverse J-proteins were required for chaperone-dependent degradation

The HSP70 chaperone cycle oscillates between the ATP-bound form, which binds substrates with low affinity and is more accessible for substrate capture, and the ADP-bound form, which binds substrates with high affinity and is less accessible. The transition between the ATP and the ADP form is brought about by HSP70-catalyzed hydrolysis of bound ATP, which is enhanced by cochaperones called J-proteins (Kampinga and Craig, 2010). We and others have observed a role for J-proteins in protein degradation, but a consensus is lacking on which particular species is most important, if there is indeed only one (Heck *et al.*, 2010; Park *et al.*, 2013; Summers *et al.*, 2013). In contrast to the highly uniform action of Sse1 or HSP70, the J-proteins show a remarkable variety of roles in the degradation of distinct substrates (Heck *et al.*, 2010; Park *et al.*, 2013; Summers *et al.*, 2013). We first focused on Ydj1, a J-protein with broad functions and significance in the degradation of some short-lived and abnormal proteins in yeast (Lee *et al.*, 1996). We had previously studied this dependency with the *ydj1*Δ null mutation (Heck *et al.*, 2010). However, this slow-growing yet viable null rapidly develops several suppressors, and phenotyping with this strain is subject to highly variable outcomes. Furthermore, Ydj1 is often redundant with the related J-protein Hlj1, which is null-viable and not compromised for growth (Sahi and Craig, 2007). Accordingly, the best test of dependence for Ydj1 is to employ the *ydj1-151hlj1*Δ double mutant (Youker *et al.*, 2004). The results from testing this strain were revealing. For three of our test substrates, the effects of the double mutant were highly varied. tGnd1-GFP was strongly stabilized, while stGnd1 was partially stabilized and Δss-CPY*-GFP was actually degraded more rapidly (Figure 2C). Thus, the role of J-proteins during CQC is complex and substrate-dependent.

Because a Gnd1 truncation similar to stGnd1 has been reported to undergo ribosome-associated degradation by Ubr1 (Verma *et al.*, 2013), we examined the contribution of ribosome-associated J-proteins in the degradation of stGnd1. The principal J-proteins at the fore are Jjj1 and Zuo1. stGnd1 was stabilized in *jjj1*Δ and *zuo1*Δ (Figure 2D), indicating that both of these J-proteins play a partial role. Consistent with this result, removal of the non-ATP–hydrolyzing ribosomal HSP70, Ssz1 (Huang *et al.*, 2005), also strongly stabilized stGnd1. Again, the effects were highly substrate specific: while the *ssz1*Δ null strain blocked stGnd1 degradation, it had little or no effect on degradation of tGnd1-GFP or Δss-CPY*-GFP.

We then examined the J-protein Sis1, which strongly stabilizes Δss-CPY*-GFP (Park *et al.*, 2013). Because the *sis1*Δ null is lethal, we employed a previously reported strain where tetracycline-suppressible promoter is used for lowering Sis1 activity (Aron *et al.*, 2007;

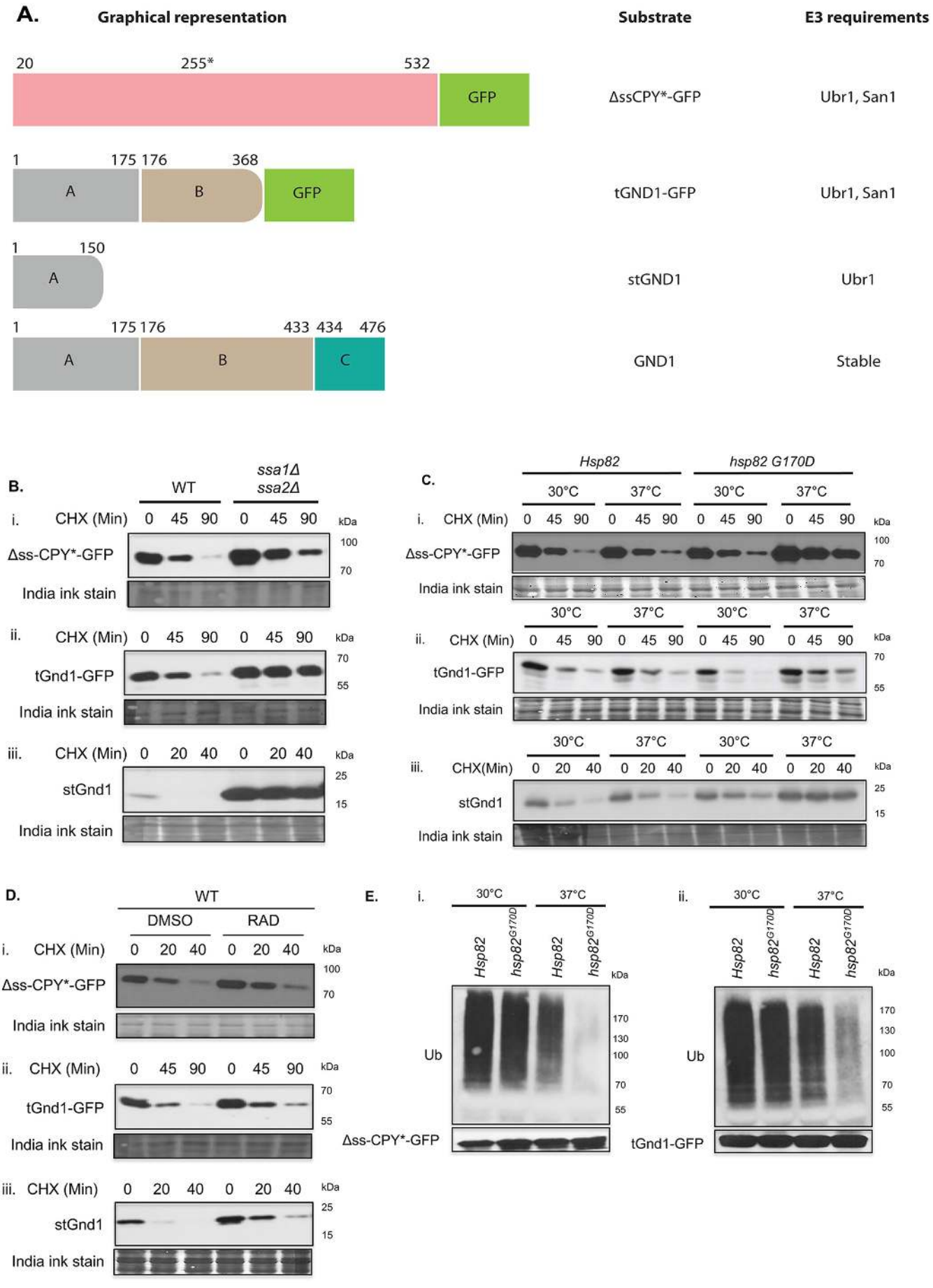
A.
Graphical representation
Substrate
E3 requirements
20
255*
532
GFP
ΔssCPY*-GFP
Ubr1, San1
1
175 176
368
A
B
GFP
tGND1-GFP
Ubr1, San1
1
150
A
stGND1
Ubr1
1
175 176
433 434
476
A
B
C
GND1
Stable
B.
WT
ssa1Δ ssa2Δ
i. CHX (Min) 0 45 90 0 45 90 kDa
Δss-CPY*-GFP
India ink stain
100
70
ii. CHX (Min) 0 45 90 0 45 90 kDa
tGnd1-GFP
India ink stain
70
55
iii. CHX (Min) 0 20 40 0 20 40 kDa
stGnd1
India ink stain
25
15
C.
Hsp82
hsp82 G170D
30°C
37°C
30°C
37°C
i. CHX (Min) 0 45 90 0 45 90 0 45 90 0 45 90 kDa
Δss-CPY*-GFP
India ink stain
100
70
ii. CHX (Min) 0 45 90 0 45 90 0 45 90 0 45 90 kDa
tGnd1-GFP
India ink stain
70
55
iii. CHX(Min) 0 20 40 0 20 40 0 20 40 0 20 40 kDa
stGnd1
India ink stain
25
15
D.
WT
DMSO
RAD
i. CHX (Min) 0 20 40 0 20 40 kDa
Δss-CPY*-GFP
India ink stain
100
70
ii. CHX (Min) 0 45 90 0 45 90 kDa
tGnd1-GFP
India ink stain
70
55
iii. CHX (Min) 0 20 40 0 20 40 kDa
stGnd1
India ink stain
25
15
E.
i.
30°C
37°C
Hsp82
hsp82G170D
Hsp82
hsp82G170D
kDa
Ub
Δss-CPY*-GFP
170
130
100
70
55
ii.
30°C
37°C
Hsp82
hsp82G170D
Hsp82
hsp82G170D
kDa
Ub
tGnd1-GFP
170
130
100
70
55

Park *et al.*, 2013, 2017). We found that the constitutively expressed Tet-promoter Sis1 strains, without addition of doxycycline, already had demonstrably lower levels of the Sis1 protein by immunoblotting (Supplemental Figure 3; Walters *et al.*, 2015). These strains show strong stabilization of both Δss-CPY*-GFP and tGnd1-GFP, in contrast to the *ydj1-151hlj1*Δ mutant, which enhances degradation of the former but strongly stabilized the latter (Figure 2E, i and ii). Degradation of stGnd1 was also affected by the loss of Sis1 (Figure 2Eiii). Interestingly, application of doxycycline, which further depleted Sis1, partially *alleviated* the degradation defect of the stabilized substrates. This result may reflect a compensatory up-regulation of other J-proteins in the face of the added stress of further Sis1 depletion.

Parsing the functions of Sis1 in degradation

Most of San1 substrates that have been studied are cytoplasmic, and it is not known how they are localized to the nucleus and how chaperones are involved in the process (Amm and Wolf, 2016; Jones *et al.*, 2020). Δss-CPY*-GFP is partially San1-dependent for its degradation, and the role of Sis1 in its degradation was first described by the Hartl group (Max Planck Institute of Biochemistry) and is confirmed in Figure 2 (Park *et al.*, 2013). We previously showed that HSP70 is involved in the nuclear transport of this substrate and ubiquitination by the resident QC ligase San1 (Heck *et al.*, 2010). Because San1 can ubiquitinate substrates with varying dependence on chaperones (Guerriero *et al.*, 2013; Jones *et al.*, 2020), we sought to better understand the role of Sis1 in degradation of this substrate, with particular interest in its role in ligase action versus nuclear transport. Accordingly, we examined a variant of Δss-CPY*-GFP with an appended nuclear exclusion signal (NES; Δss-CPY*-GFP+NES). This variant is efficiently excluded from the nucleus (Park *et al.*, 2013), and—as expected from the cellular residence of one of the principal ligases involved in its degradation (i.e., San1)—the substrate was subject only to Ubr1-mediated degradation (Heck *et al.*, 2010). Degradation was also no longer dependent on San1, consistent with nuclear exclusion (Supplemental Figure 4). We then examined the effect of lowered Sis1 activity on this Ubr1-only substrate. Sis1 depletion caused a degree of stabilization, but the effect was not as dramatic as on the native substrate (Δss-CPY*-GFP), which underwent mainly San1-dependent destruction. Further lowering the levels of Sis1 by the addition of doxycycline did not enhance the effect on cytosolic Δss-CPY*-GFP+NES (Figure 2Fi).

The data presented above indicate the notable Sis1 dependence of Δss-CPY*-GFP degradation in the nucleus, which is related to its requirement for San1. To discern whether the role of Sis1 was linked to San1-mediated degradation, or in delivery to San1 in the nucleus, we coexpressed a cytosol-restricted version of San1-NLS with the cytosolic Δss-CPY*-GFP+NES to remove the nuclear transport requirement. As expected from our earlier studies (Heck *et al.*, 2010), this version of San1 dramatically accelerated the degradation of the cytosolic construct (Figure 2Fii). However, the action of San1 was unaffected by lowered Sis1 activity, despite the strong effect of low Sis1 on Δss-CPY*-GFP. These data indicate that Sis1 has at least two functions in cytoplasmic degradation. First, it helps deliver substrates to nuclear-localized San1, consistent with the role of HSP70 described in our previous studies. Second, Sis1 contributes directly to Ubr1-mediated degradation, as observed with the cytoplasmic Δss-CPY*-GFP substrate.

Distinct J-proteins can allow Ubr1-mediated ubiquitination of a single substrate

The Ubr1-specific substrate stGnd1 showed a surprisingly complex dependence on two classes of J-proteins. Along with the strong dependence on the redundant pair of ribosome-associated Zuo1 and Jjj1 (Figure 2D), removal of Ydj1 also caused partial substrate stabilization (Figure 2C). To further define how these distinct J-proteins function, we studied the ubiquitination of stGnd1 in vitro, using a bound substrate assay developed previously (Heck *et al.*, 2010). FLAG-tagged stGnd1 (fl-stGnd1) was immunoprecipitated from the lysate of a *ubr1*Δ strain with anti-FLAG M2 beads. The substrate was then incubated with cytosolic fractions from WT or the desired mutants in the presence or absence of ATP, followed by SDS–PAGE and immunoblotting for the presence of substrate and ubiquitin conjugation.

We found that bead-bound fl-stGnd1 was ubiquitinated in an ATP-dependent manner, showing high dependence on the presence of the substrate (Figure 3A). We then compared the effects of *ubr1*Δ and *san1*Δ on the level of ubiquitination. As was the case in vivo, only loss of Ubr1 returned ubiquitination to background levels. In contrast, *san1*Δ cytosol supported in vitro stGnd1 ubiquitination at levels comparable to those of WT (Figure 3A). Thus, the stringent in vivo Ubr1 specificity of stGnd1 was preserved in the in vitro substrate capture assay. We have shown earlier that HSP70 was also required for ubiquitination (Figure 3B; Heck *et al.*, 2010). A single mutation

FIGURE 1: HSP70 and HSP90 are required for degradation of several CQC substrates. (A) CQC substrates used herein, with names and main E3 ligases responsible for degradation in yeast, as described (Heck *et al.*, 2010; Park *et al.*, 2013). Δss-CPY*-GFP is the ERAD substrate CPY* with the signal sequence removed and GFP appended. tGnd1-GFP and stGnd1 are CQC substrates derived from stable full-length Gnd1 (476 aa). tGnd1-GFP is truncated at residue 368 with GFP appended. stGnd1 is truncated at residue 150. (B) Ubr1-mediated CQC was slowed in *ssa1*Δ*ssa2*Δ cells expressing the indicated substrates. Log-phase cultures were subjected to CHX chase for the indicated times, followed by lysis and substrate immunoblotting to evaluate stability. Growth and incubation were at 30°C, and incubation temperatures were as indicated. (C) HSP90 requirement was tested with HSP90 null strains (*hsp82*Δ*hsc82*Δ) expressing either WT *HSP82* or temperature-sensitive *hsp82*G170D alleles. Strains with the indicated CQC substrate were grown at the permissive temperature of 30°C and either maintained at 30°C or shifted to 37°C for 1 h as indicated; followed by CHX chase as in B. (D) HSP90 requirement was tested using the HSP90 inhibitor RAD. WT cells expressing the indicated substrates were treated with DMSO or 100 μM RAD for 60 min followed by CHX chase. (E) HSP90 was required for in vivo CQC substrate ubiquitination. HSP90 strains in C were grown at a permissive temperature of 30°C and either maintained at 30°C or shifted to 37°C for a 1 h incubation. Cells were then lysed and subjected to substrate IP followed by immunoblotting for ubiquitin (top panels) or substrate (bottom panel). Bottom panels show Δss-CPY*-GFP or tGnd1-GFP in 10% of the lysate used for the IP. The 1 h incubation temperatures employed in each culture (30°C and 37°C) are shown. Anti-GFP antibody was used to detect Δss-CPY*-GFP and tGND1-GFP while stGND1 levels were detected using anti-HA. Anti-ubiquitin antibody was used to detect substrate ubiquitination. India ink–stained blots were used to assess loading.

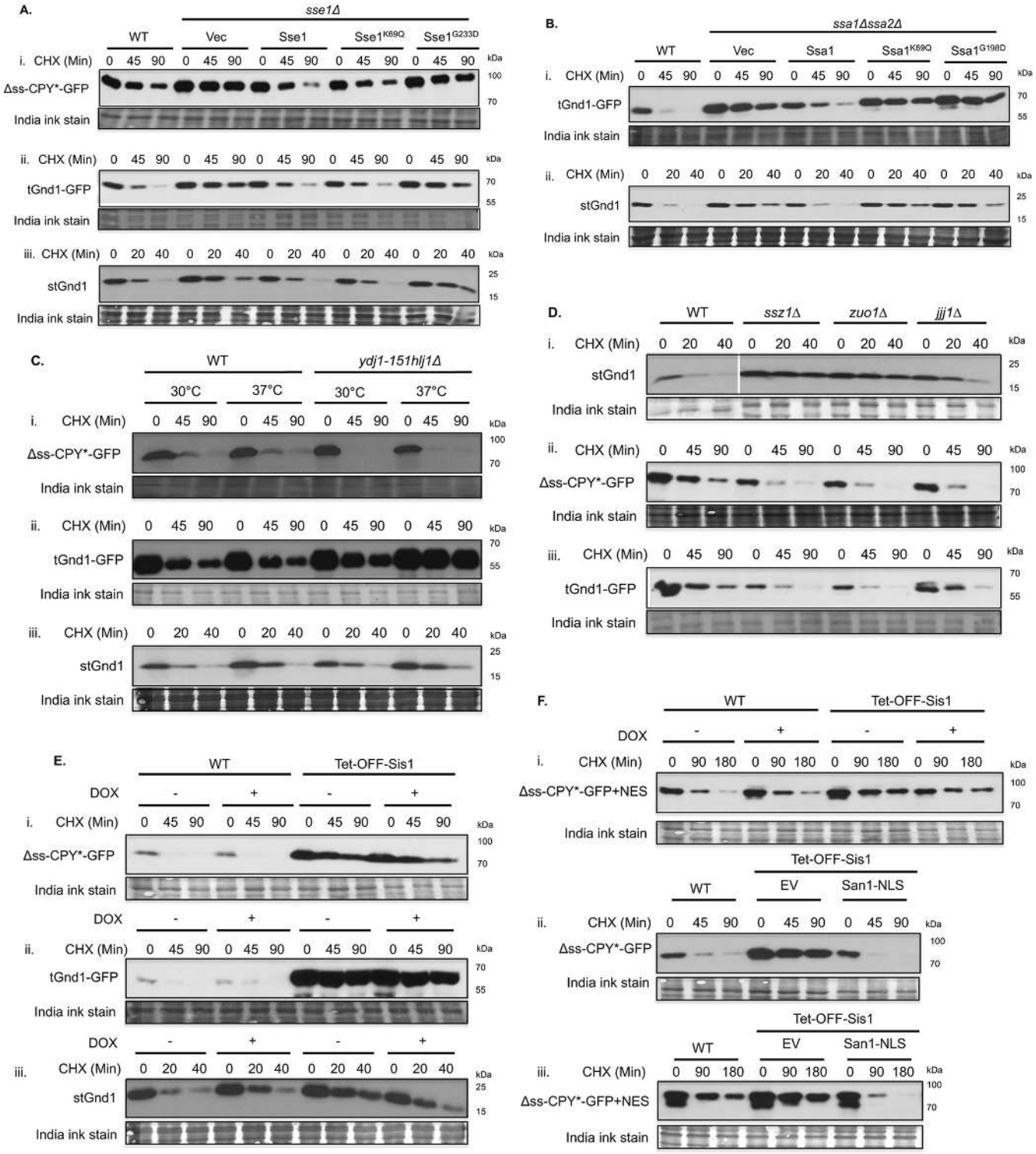

FIGURE 2: ATP involvement in CQC. (A) Sse1 nucleotide exchange activity was required for CQC. *sse1*Δ cells expressing the indicated substrate and the indicated Sse1 variants Sse1 (WT), Sse1^{K69Q} (ATP hydrolysis deficient), or Sse1^{G233D} (ATP binding deficient) were subjected to CHX chase and substrate immunoblotting as described. (B) HSP70 ATP hydrolysis was required for CQC. WT or *ssa1*Δ*ssa2*Δ cells expressing the indicated substrate and HSP70 variants Ssa1 (WT), Ssa1^{K69Q} (ATP hydrolysis deficient), or Ssa1^{G198D} (ATP binding deficient) were subjected to CHX chase as indicated. (C) Ydj1 and Hlj1 J-proteins had varied effects on substrate CQC. WT or *ydj1-151hlj1*Δ cells expressing the indicated substrates were subjected to CHX chases at 30°C or 37°C as indicated. The indicated temperatures were imposed for 1 h before and during CHX chase. (D) J-proteins Zuo1, Jjj1, and Ssz1 were involved in stGnd1 degradation. WT, *zuo1*Δ, *jjj1*Δ, and *ssz1*Δ strains expressing the indicated substrates were subjected to CHX chase and substrate immunoblotting as described. Supplemental Figure 2 shows the uncropped image for the stGND1 immunoblot. (E) Sis1 involvement in CQC. WT and Tet-OFF-Sis1 cells expressing the indicated substrates were grown at 30°C and treated with 10 μM doxycycline or vehicle for 20 h followed by CHX chases for the indicated times. Also see Supplemental

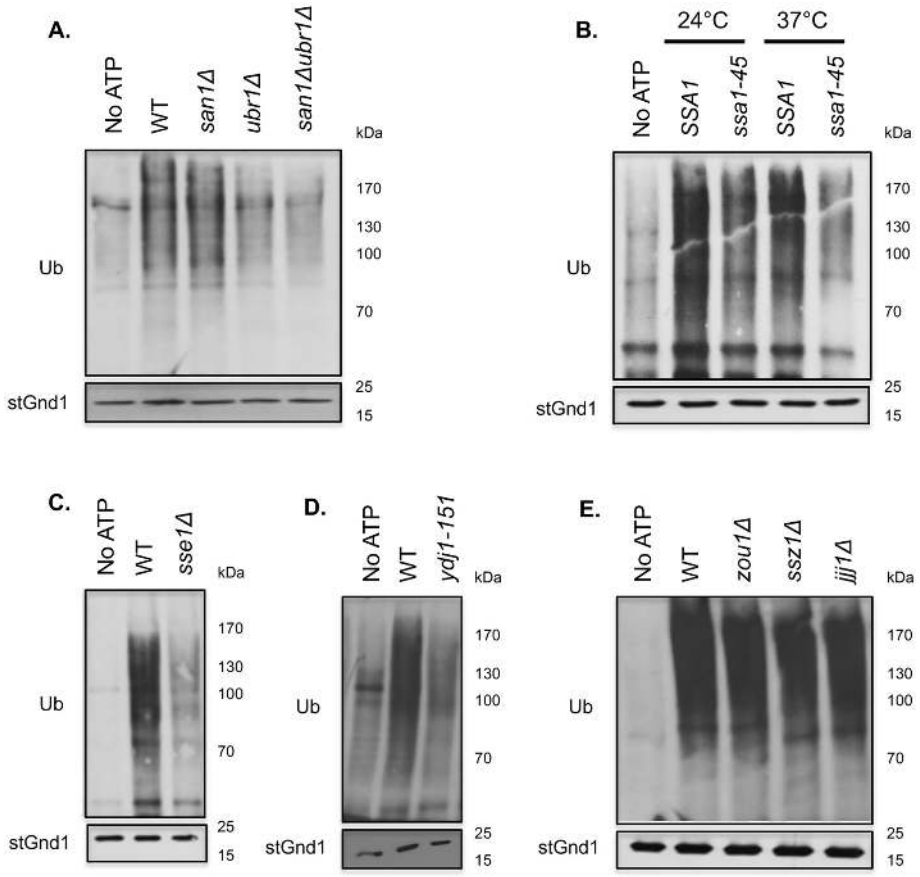

FIGURE 3: In vitro ubiquitination of immunocaptured stGnd1. Cytosols were prepared from the indicated strains and used for in vitro ubiquitination of fl-stGnd1 as described in *Materials and Methods*: lysates from a *ubr1*Δ null strain expressing fl-stGnd1 were subjected to FLAG bead IP followed by incubation of bead-immobilized substrate in the indicated WT or mutant cellular lysates, with or without ATP, to evaluate effects on ubiquitination. Beads were then washed and subjected to immunoblotting for ubiquitin or unmodified stGnd1 as indicated. fl-stGnd1 beads (20 µl) were used for reaction in the presence of the indicated cytosols at 30°C for 40 min in the absence (No ATP) or presence of 7.5 mM ATP. (A) Ubr1 was the sole ligase responsible for stGnd1 ubiquitination. Cytosols from isogenetic WT, *san1*Δ, *ubr1*Δ, or *san1*Δ*ubr1*Δ cells were used for the reactions. (B) In vitro stGnd1 ubiquitination required Ssa1. Cytosols from *Ssa1* and *ssa1-45* cells were prepared after a 1 h temperature shift to 37°C. (C) Sse1 was required for stGnd1 ubiquitination. Cytosols were prepared from isogenetic WT and *sse1*Δ cells. (D) Ydj1 was necessary for stGnd1 ubiquitination in vitro. Cytosols were prepared from WT and *ydj1-151ydj1*Δ*hlj1*Δ cells, and reactions were performed as described. (E) The ribosome-associated proteins were dispensable for stGnd1 ubiquitination. Cytosols were prepared from WT cells and those lacking Zuo1, Jjj1, and Ssz1. Anti-FLAG antibody was used for detecting stGND1, and anti-ubiquitin antibody was used to detect ubiquitination. Bottom panels in all the figures show the input levels of fl-stGnd1.

(P417L) renders Ssa1 temperature sensitive (*ssa1-45* allele), affecting ATP cycling and specific chaperone functions (Needham *et al.*, 2015). While *SSA1* cytosols prepared from cells pretreated at 24°C or 37°C supported stGnd1 ubiquitination, there was a substantial decrease in ubiquitination of fl-stGnd1 when tested with *ssa1-45* cytosol from cells preincubated at 37°C (Figure 3B). Similarly, the strong dependence on the NEF Sse1 was also recapitulated (Figure 3C). In vitro stGnd1 ubiquitination was partially dependent on Ydj1 as indicated from the effects of *ydj1-151hjl1*Δ cytosol (Figure 3D). Conversely, cytosols from *ssz1*Δ, *zuo1*Δ, and *jjj1*Δ fully supported stGnd1 ubiquitination in vitro despite their strong role in degradation in vivo (Figure 3E). Thus, the J-protein dependence was highly condition-dependent and could be met by two distinct groups of these cochaperones. One model for this behavior is that the primary detection of stGnd1 occurs cotranslationally and is thus mediated by ribosome-associated J-proteins that assist HSP70. stGnd1 that escapes ribosomal detection is then subjected to Ydj1-dependent degradation. Since immunoprecipitated stGnd1 has been released into the soluble pool, Ydj1 was the preferred J-protein for HSP70-dependent ubiquitination.

Taken together, these results implicate a role for the HSP70 ATP hydrolytic cycle in chaperone-mediated ubiquitination and degradation of cytosolic proteins. HSP70 is universally required, and both the NEF Sse1, which loads ATP onto HSP70, and the J-proteins, which promote ATP hydrolysis, contribute to this process. Furthermore, the strong dependence on HSP90 and inhibition by RAD implicates HSP90-mediated ATP hydrolysis in CQC. Two key questions emerge from these studies: 1) does either HSP70 and HSP90 function directly in substrate ubiquitination, or at later steps? And 2) are the chaperone ATP hydrolytic cycle(s) directly required for ubiquitination itself, or rather involved in less direct aspects such as substrate state or localization? It is clear from our work and several other studies that the physical state and the compartmental fate of misfolded chaperone clients could be a strong, or even the principal, determinant for chaperone requirements in degradation. For example, the role of HSP70/Sis1 in Δss-CPY*-GFP degradation is due to delivery of this San1-dependent substrate to the nucleus. Similarly, since chaperones can contribute to both substrate

Figure 3. (F) Role of nuclear transport in Sis1-mediated CQC. (i) WT and Tet-OFF-Sis1 cells expressing Δss-CPY*-GFP+NES were grown at 30°C and treated with 10 µM doxycycline or vehicle for 20 h followed by CHX chases for the indicated times. Also see Supplemental Figure 4. Cytoplasmic San1 degraded both Δss-CPY*-GFP and CPY*-GFP +NES independent of Sis1 function. Tet-OFF-Sis1 cells expressing Δss-CPY*-GFP (ii; top) or Δss-CPY*-GFP+NES (iii; bottom) and cytoplasmic San1 variant HSV-San1-NLS or empty vector and corresponding WT cells expressing Δss-CPY*-GFP and Δss-CPY*-GFP+NES are shown in the left panels for comparison. CHX chase was performed for the indicated times without addition of any doxycycline. Anti-GFP antibody was used to detect Δss-CPY*-GFP, Δss-CPY*-GFP+NES, and tGND1-GFP while anti-HA was used to detect levels of stGND1. Bottom panels depict India ink–stained blots for all samples to assess equal loading.

solubility and disaggregation, it is unclear how direct an apparently strong chaperone effect is in the E3 catalytic process when studied in intact cells. Accordingly, we developed a novel approach using bead-immobilized misfolded substrate to obviate some of these issues and address the extent to which each chaperone class was directly involved in E3 QC.

A bead-immobilized substrate assay for studying chaperone-dependent ubiquitination

As one way to remove the variables associated with substrate solubility or transport in vivo, we modified the in vitro ubiquitination protocol to create a bead-based assay with a covalently immobilized QC substrate. Specifically, we employed commercially available immunoglobulin G (IgG) agarose beads with bound rabbit IgG. Because protein QC can be specific for structural rather than sequence-specific features (Chen *et al.*, 2011; Rosenbaum *et al.*, 2011; Fredrickson *et al.*, 2013; Jones *et al.*, 2020), we posited that the use of a mammalian protein as a misfolded substrate would not hamper the recognition of misfolding hallmarks by the yeast machinery. This trans-species leniency has been useful in studying yeast QC with other mammalian misfolded proteins such as VHL, FUS, TDP43, and Htt (McClellan *et al.*, 2005; Sun *et al.*, 2011; Park *et al.*, 2013; Samant *et al.*, 2018). However, because the substrate protein (mature IgG) in this case is covalently linked to the beads, any effects arising from substrate solubilization or transport would be obviated. In this way, we could examine the degree to which chaperones (or any examined component) are directly involved in CQC ubiquitination. Furthermore, this approach enabled biochemical manipulations not possible in vivo. The assay was run with covalent IgG beads in either a native (N) or denatured (D) state in the presence of yeast cytosol, followed by liberation of ubiquitinated, disulfide-linked IgG subunits from bead-linked heteromeric partners. The liberated ubiquitinated IgG molecules are then analyzed by SDS–PAGE followed by immunoblotting to detect multiubiquitin conjugates (Figure 4A).

We first established that bead-bound IgG would undergo misfolding-dependent ubiquitination when incubated with yeast cytosol, which was prepared as described (Heck *et al.*, 2010). Indeed, treatment of the beads with the denaturant guanidinium hydrochloride (GdHCl) brought about an increase in ATP-dependent ubiquitination (Figure 4, B and C). The effect of GdHCl on ubiquitination reached a maximum after 30–40 min of incubation (Figure 4C). As expected from our earlier ERAD and substrate capture assays in the presence of yeast cytosol (Nakatsukasa *et al.*, 2008; Garza *et al.*, 2009; Heck *et al.*, 2010; Vashistha *et al.*, 2016), immobilized substrate ubiquitination was ATP-dependent (Figure 4D). In addition, since IgG consists of heavy and light chains connected by disulfide bonds, the subunits are connected to the agarose beads either by the chemical cross-linker or by disulfide bonds to subunits that are in turn chemically cross-linked to the beads. Accordingly, we expected that ubiquitinated IgG subunits would be freed from the beads and detected only by breaking the disulfide bonds, which was indeed the case. Figure 4E shows identical reaction samples of denatured IgG beads in which the sample buffer contained or lacked dithiothreitol (DTT). Thus, the immobilized QC substrate was covalently linked to the beads during the reaction, removing any effects of substrate solubilization or liberation that may be brought about by chaperones or other factors when the substrates are not constrained. This approach also works with heat denaturation (Heck, 2010), but we found that the use of GdHCl was more reproducible and it was easier to control induced misfolding by use of a soluble molecule. Accordingly, the studies below focus on that approach.

Ubr1 was required for bead-immobilized QC ubiquitination

We first tested the role of the two principal CQC E3 ligases in the ubiquitination of bead-bound misfolded IgG. Cytosols prepared from otherwise isogenetic WT or *ubr1*Δ, *san1*Δ, and *ubr1*Δ*san1*Δ mutant strains were prepared and tested for their ability to support bead-bound ubiquitination. There was a striking decrease in IgG ubiquitination when both ligases were absent in the cytosols from a double null strain (Figure 4F). By comparing the WT signal to the single *san1*Δ or the *ubr1*Δ cytosols, the contribution to the reaction by Ubr1 or San1, respectively, was evaluated. In several repetitions of the experiment, use of a double null *ubr1*Δ*san1*Δ cytosol did not support denaturation-specific ubiquitination at all. The majority of the ubiquitination activity was due to Ubr1, as indicated by comparing a suite of mutant cytosols. The contribution of San1 was somewhat variable between reactions (e.g., compare Figures 4F and 5C) but typically was ~10%. The variability probably emerged from the appearance of San1 in the cytosolic fraction during cytosol preparation in the case of the WT strains. These results indicate that the dual dependence on these two distinct but similarly purposed ligases seen in vivo was preserved in vitro, with Ubr1 contributing the majority of activity toward ubiquitination of immobilized misfolded IgG.

Immobilized IgG ubiquitination required the HSP70 ATP hydrolysis cycle

By comparing the effects of otherwise isogeneic cytosols prepared from *SSA1* or *ssa1-45* strains, we next tested for the HSP70 dependence in bead-bound substrate ubiquitination. Cytosols prepared from *ssa1-45* yeast that had been preincubated at the nonpermissive temperature were deficient for misfolded IgG ubiquitination (Figure 5A). We next confirmed Ssa1 dependence by plasmid complementation. We introduced the empty plasmid or plasmids containing Ssa1 or Ssa1^{K69Q} into *ssa1-45* strains and utilized the resulting cytosols in a bead-based ubiquitination assay. Cytosol prepared from the *ssa1-45* strain carrying the Ssa1 plasmid supported ubiquitination, while the *ssa1-45* strain carrying the empty plasmid or Ssa1^{K69Q} allele did not support ubiquitination (Figure 5B). Consistent with our results presented above, these data indicate that HSP70 is required for Ubr1-mediated ubiquitination of bead-immobilized substrate, thus indicating a direct role of Hsp70 in Ubr1-mediated QC. Furthermore, the inability of the Ssa1^{K69Q} mutant to support ubiquitination indicates that ATP hydrolysis is required. This feature was further tested below by examining the proteins that regulated the ATPase cycle and by capitalizing on specific biochemical features of HSP70 ATP hydrolysis that can be tested only in vitro.

Sse1 was required for immobilized misfolded substrate Ubr1-mediated ubiquitination

We next evaluated the involvement of Sse1 in the assay. We had previously reported that the absence of Sse1 causes a poorly characterized activation of San1 in a similar in vitro assay (Heck *et al.*, 2010), which obscures the analysis of Sse1 in Ubr1-mediated ubiquitination. To study the role of Sse1 in this bead-bound assay without this interfering activity, we employed *san1*Δ null strains to allow unambiguous observation of the Ubr1-mediated component, which is both the major activity in this assay and more important physiologically during cytoplasmic stress (Heck *et al.*, 2010; Theodoraki *et al.*, 2012). Bead-bound ubiquitination was identical to that of the WT when using *san1*Δ cytosol but strongly diminished in *san1*Δ*sse1*Δ cytosol, indicating the expected strong dependence of Ubr1-mediated ubiquitination on Sse1 (Figure 5C). We next employed the *san1*Δ*sse1*Δ strain to test the functional requirements for Sse1 in the

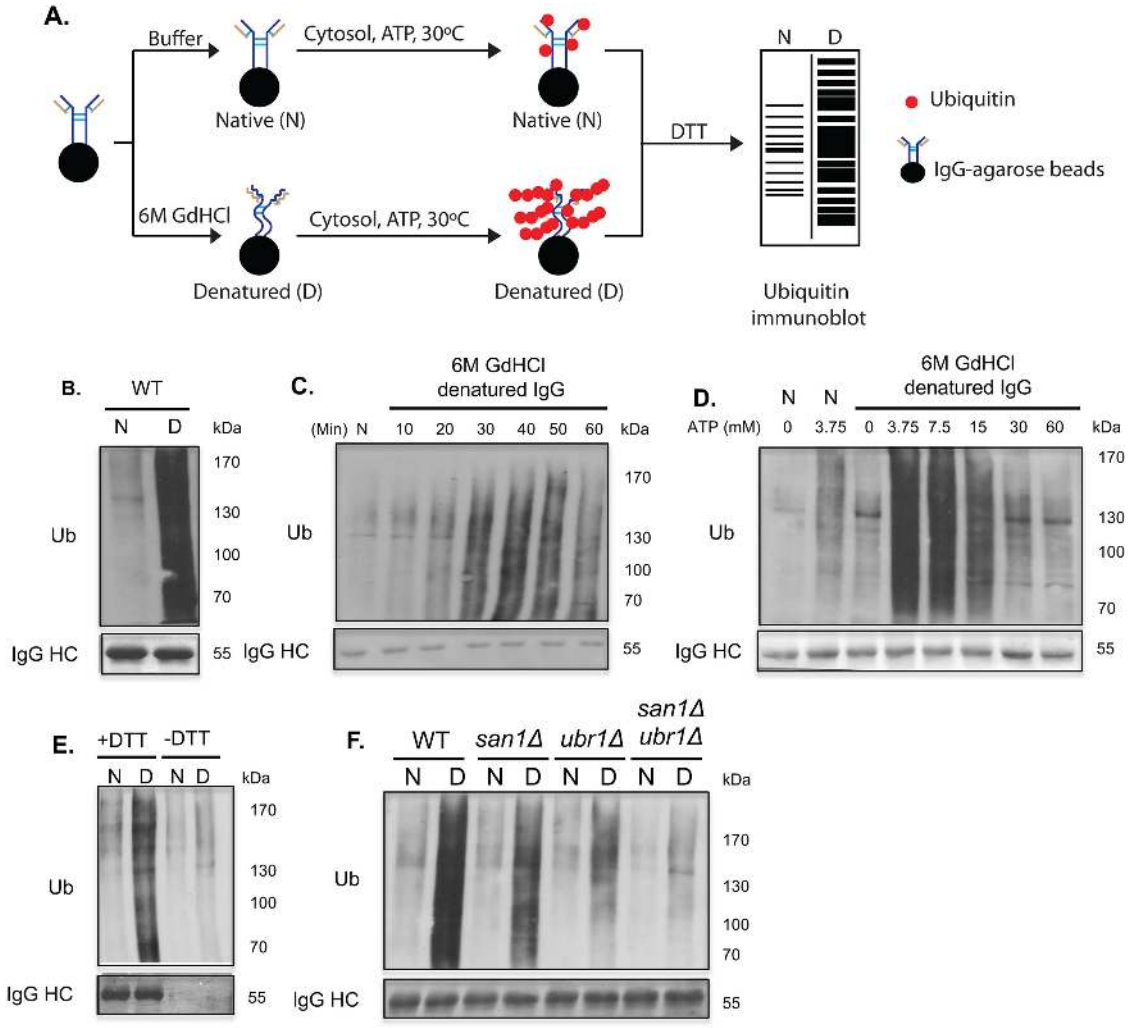

FIGURE 4: Bead-immobilized substrate ubiquitination assay. (A) Schematic depicting the bead-based ubiquitination assay. IgG beads were treated with buffer (N) or 6 M GdHCl (D) at 4°C for 20 min and washed with buffer for use in assays. (B) Denatured IgG was ubiquitinated by WT cytosol. Samples were removed, and the reaction was stopped by aspirating the cytosol, washing three times with IP wash buffer, and finally adding urea sample buffer. Total cytosolic protein (150 µg) is used in all the reactions in the presence of 7.5 mM ATP and incubated at 30°C for 40 min. (C) Bead-based substrate ubiquitination time course. The reactions were performed at 30°C for the indicated times in the presence of 7.5 mM ATP. (D) Substrate ubiquitination was ATP-dependent. Reactions were performed in the absence or presence of different concentrations of ATP and were incubated for 40 min at 30°C. (E) Liberation of bead-based substrate ubiquitination reaction products was DTT-dependent. Ubiquitination signal was detected only when DTT was included in the buffer, indicating that IgG chains were released by breaking of disulfide linkages holding IgG subunits to covalently bound subunits. +DTT represents IgG beads to which buffer containing 200 mM DTT was added, –DTT represents IgG beads to which buffer lacking DTT was added. (F) Ubr1 involvement in bead-bound substrate ubiquitination. Beads were subjected to ubiquitination assays as in A with cytosols from the indicated E3 nulls. All reactions were performed at 30°C. Anti-ubiquitin antibody was used to detect ubiquitination. Bottom panels show IgG heavy chain (IgG-HC) on India ink–stained blots.

bead assay by testing cytosol from *san1Δsse1Δ* strain expressing the Sse1 mutants used earlier (Figure 2B). The Sse1 mutant that binds ATP ($Sse1^{K69Q}$) but does not hydrolyze still supported Ubr1-mediated ubiquitination, whereas the mutant that does not bind ATP ($Sse1^{G233D}$) and does not form a complex with HSP70 was able to support ubiquitination to a lesser extent (Figure 5D). Taken together, these results indicated that HSP70 and Sse1 are directly involved in Ubr1-mediated ubiquitination of misfolded proteins, despite the substrate being covalently constrained.

Since the canonical HSP70 ATPase cycle was involved in QC ubiquitination in intact cells, we next evaluated the role of HSP70-mediated ATP hydrolysis in the immobilized substrate assay. One of the features of our (and related; Garza *et al.*, 2009) versions of in vitro ubiquitination assays is that exogenous ATP must be added to support ubiquitination. Thus, nucleotide potency and specificity can be evaluated by direct addition of the appropriate analogues. We capitalized on a feature of ubiquitin biochemistry that allows unambiguous inhibition of chaperone-mediated ATP hydrolysis in a ubiquitination assay. Although ubiquitination requires ATP hydrolysis for the activation of ubiquitin by the E1 ubiquitin-activating enzyme, the E1 enzyme hydrolyzes ATP to form AMP as a leaving group, which drives formation of the E1 thiolester bond (Walden *et al.*, 2003).

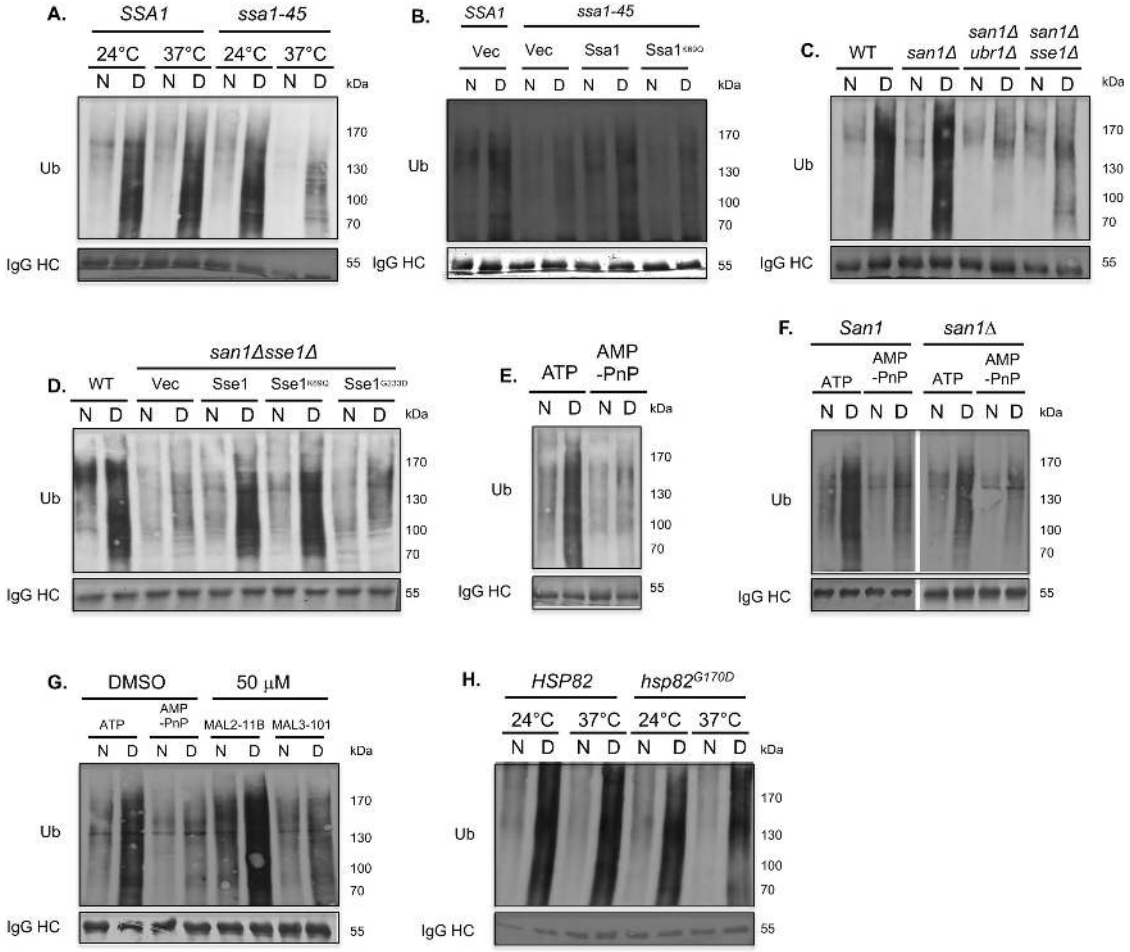

FIGURE 5: Involvement of chaperones in bead-immobilized substrate ubiquitination assay. (A) HSP70 was required for bead-based ubiquitination. Ubiquitination assays were performed with WT or *ssa1-45* ts cytosols at 30°C. Temperatures above lanes indicate 1-h pretreatment of intact cells before cytosol preparation. (B) Bead-immobilized substrate ubiquitination assay requires HSP70 ATP hydrolysis. Ubiquitination assays were performed with WT or *ssa1-45* ts strains transformed with either vector, SSA1 or SSA1^{K69Q} plasmids. Cytosols were prepared after growing the cells at 37°C for 1 h. Only cytosol prepared from cells carrying the SSA1 plasmid was able to complement ubiquitination while SSA1^{K69Q} was not able to. (C) Sse1 was required for Ubr1-mediated bead-bound ubiquitination. *san1*Δ strains were evaluated for Ubr1- and Sse1-dependence by use of the indicated cytosols in the reaction mixes. (D) Ubr1-dependent bead-bound ubiquitination required Sse1 nucleotide exchange activity. Ubiquitination reactions were performed using cytosols from *sse1*Δ*san1*Δ strains expressing the indicated Sse1 variants Sse1 (wt), Sse1^{K69Q} (ATP hydrolysis deficient), or Sse1^{G233D} (ATP binding deficient). (E) Bead-bound ubiquitination was not supported by AMP-PnP. Ubiquitination assays with WT cytosol in the presence of 7.5 mM ATP or AMP-PnP. (F) Ubr1-dependent ubiquitination was not supported by AMP-PnP. Cytosols were prepared from WT or *san1*Δ cells and used for bead-bound ubiquitination in the presence of ATP or AMP-PnP. (G) Pharmacological inhibition of J-proteins (Hsp40) affected bead-based substrate ubiquitination. WT cytosol was treated with an inactive control, MAL2-11B, J-protein inhibitor MAL3-101, or vehicle (2.5% [vol/vol] DMSO) for 20 min on ice and subsequently used for bead-based substrate ubiquitination. An additional reaction was performed in the presence of AMP-PnP as a positive control. (H) Bead-bound ubiquitination was HSP90-independent. Ubiquitination was performed with cytosol from HSP90 null strains (*hsp82*Δ*hsc82*Δ) expressing either WT HSP82 or the temperature-sensitive hsp82^{G170D} allele. Strains were grown at the permissive temperature of 30°C and either maintained at 30°C or shifted to 37°C for a 1 h preincubation, as indicated above the lanes. All reactions were performed at 30°C. Anti-ubiquitin antibody was used to detect ubiquitination. Bottom panels show IgG heavy chain (IgG-HC) on India ink–stained blots.

Conversely, HSP70 hydrolyzes the γ-phosphate in ATP in the course of its action. Thus, appropriate use of the nonhydrolyzable analogue, β,γ-imidoadenosine 5-triphosphate (AMP-PnP), which supports ubiquitination but not the chaperone ATPase activity, will specifically report on chaperone-dependent hydrolytic events. We found that AMP-PnP could not support ubiquitination of denatured IgG (Figure 5E), lowering the degree of ubiquitination to that seen in the absence of the ligases. To ensure that the Ubr1 component was specifically dependent on γ-phosphate release, we repeated the experiment in a *san1*Δ background, and confirmed that the majority of the Ubr1-dependent ubiquitination was dependent on ATP hydrolysis at the γ position (Figure 5F). Importantly, the concentration of AMP-PnP used fully supported global cytosolic ubiquitination, in which ATP-dependent ubiquitination by a wide variety of other ligases was evaluated by immunoblotting of a sample of the cytosolic reaction mix for ubiquitin (Supplemental Figure 5).

J protein–facilitated bead-bound substrate ubiquitination

Ubiquitination of bead-bound IgG required HSP70, Ubr1, Sse1, and ATP hydrolysis. This implied that the J-protein cochaperones would also be involved in chaperone-dependent ubiquitination. As detailed earlier, the J-protein requirement in the in vivo and substrate capture assays was clear but also complex: different substrates showed strikingly varied dependencies, as might be expected for this large family of cochaperones that can exhibit redundant functions, are contraregulated, and promote specificity during HSP70-dependent processes (Kampinga and Craig, 2010). There are 23 J-proteins in yeast (Sahi and Craig, 2007), and we tested all the cytoplasmic J-proteins as either single or double nulls as sources for cytosol to assess their ability to support bead-bound substrate ubiquitination (unpublished data). None of the cytosols had any effect on this assay. As an alternative approach, we examined the J-protein contribution pharmacologically and capitalized on a family of compounds that modulate J protein–mediated stimulation of HSP70 ATP hydrolysis (Fewell *et al.*, 2004; Wisén *et al.*, 2010; Huryn *et al.*, 2011; Terrab and Wipf, 2020). MAL3-101 specifically inhibits J-protein–stimulated HSP70 ATPase activity (Fewell *et al.*, 2004). MAL3-101 blocked substrate ubiquitination to nearly the same extent as substituting ATP for AMP-PnP, or depleting the E3 ligases, while a structurally similar but inactive analogue, MAL2-11B, had no effect in this assay. These data indicate that J protein–catalyzed processes were also involved in ubiquitination of bead-immobilized misfolded IgG (Figure 5G). As was the case with AMP-PnP, the small molecule J inhibitor had no effect on global ubiquitination. Furthermore, the striking and specific effect of the MAL3-101 compound further supported the need for ATP hydrolysis implied by the effects of $Ssa1^{K69Q}$ mutation and AMP-PnP in the bead-based assay.

HSP90 was dispensable in bead-bound substrate ubiquitination

We developed the immobilized substrate assay to discern direct chaperone-dependent effects on ligase action as opposed to those that function at distinct parts of the UPS pathway or in a substrate physical state. Ubiquitination of IgG on beads fully recapitulated the in vivo role of HSP70s. In vivo, HSP90 was also required for the degradation of each cytoplasmic substrate tested, including both mixed Ubr1/San1 substrates like Δss-CPY*-GFP/tGnd1-GFP and a pure Ubr1 substrate, stGnd1, as queried by both genetic means and with drugs (Figure 1). Furthermore, in vivo ubiquitination assays with both the HSP90 mutant *hsp82*G170D and HSP90-inhibiting drugs uncovered a dependence on HSP90 during substrate ubiquitination (Figure 1D and Supplemental Figure 1). However, in contrast to the case with HSP70, neither a stabilizing mutant of HSP90 (*hsp82*G170D) nor application of Hsp90 inhibitors (geldanamycin and RAD) before cytosol preparation and continued during ubiquitination of bead-bound IgG had any effect. The Hsp90 inhibitor–treated cytosols were derived from cells for which a simultaneous in vivo degradation experiment confirmed that the doses were stabilizing, and the drugs were re-added to the cytosol after purification (unpublished data). Nevertheless, there was again no effect on bead-bound IgG ubiquitination and no effect on the major Ubr1-dependent component or the minor San1-dependent component of the reaction. A representative experiment is shown in Figure 5H. Thus, it appears that HSP90, while being important for in vivo degradation of cytoplasmic substrates, operates at a step in the process that is not directly related to substrate ubiquitination.

HSP70 was required for Ubr1 interaction with misfolded protein

In general, a sine qua non for E3 activity toward a targeted substrate is the interaction of the E3 with a given substrate (Metzger *et al.*, 2014). Although there can be important allosteric interactions above and beyond E3–substrate interaction, it is always the case that substrate–ligase interaction is necessary for ubiquitin transfer (Pruneda *et al.*, 2012). Because HSP70 plays a clear and direct role in misfolded substrate ubiquitination, we investigated the role of HSP70 in Ubr1-QC substrate interactions. We first tested whether HSP70 was involved in the interaction between FLAG-tagged Ubr1 and the prototypical substrate, Δss-CPY*-GFP, in a coimmunoprecipitation (co-IP) experiment using total cell lysates. Cells coexpressing FLAG-tagged-Ubr1 (fl-Ubr1) and Δss-CPY*-GFP in *SSA1* or *ssa1-45* mutant cells were subjected to IP with either anti-FLAG or anti-GFP antibody, followed by SDS–PAGE and immunoblotting to evaluate the interaction. Pull down of either Ubr1 or substrate showed evidence of interaction by co-IP. Furthermore, interaction between E3 and substrate was abrogated only when *ssa1-45* strains were preincubated at 37°C (Figure 6A; Supplemental Figure 6).

We next examined the HSP70 dependence on Ubr1–substrate interactions using the bead-bound IgG platform. Immobilized IgG provides a facile approach for studying binding interactions, since the bead-bound substrate can be rapidly separated from an assay mix and queried for associated proteins by immunoblotting. Ubr1 associated with the immobilized IgG molecules in a denaturation-dependent manner (Figure 6B; compare N to D). This interaction was HSP70-dependent since the binding of Ubr1 to the denatured (D) beads was dramatically decreased in the presence of cytosol prepared from *ssa1-45* cells expressing fl-Ubr1 and preincubated at 37°C prior to cytosol preparation (Figure 6C). The levels of both Ubr1 (Figure 6Cii) and Ssa1 (Supplemental Figure 7) were identical in all samples, independent of whether cytosols from WT or *ssa1-45* cells were used. We next evaluated the role of ATP hydrolysis in the Ssa1-dependent interaction between Ubr1 and the substrate. Surprisingly, despite the strong dependence on Ssa1 function, there was no requirement for ATP hydrolysis or exchange in Ubr1 binding to the misfolded protein (Figure 6D). AMP-PnP at concentrations that failed to support Ubr1-mediated ubiquitination, or even the complete absence of added nucleotide, had no effect on binding (Figure 6E). Similarly, loss of Sse1 had no effect on HSP70-mediated binding: cytosol prepared from a *sse1*Δ version of the *Ssa1ssa2*Δ*ssa3*Δ*ssa4*Δ strain showed unaffected Ubr1 binding to misfolded IgG (Figure 6F).

Taken together, our data indicate that the interaction of Ubr1 with misfolded proteins requires HSP70 but is independent of ATP hydrolysis or exchange. Thus, the role of HSP70 can be divided into substrate selection and substrate ubiquitination, with clearly different roles of the chaperone ATP cycle in the two phases.

DISCUSSION

The established role of classical folding chaperones in the ubiquitin-mediated destruction of misfolded proteins has given rise to the concept of "protein triage," during which chaperones can participate in both protein folding and destruction. This apparently paradoxical set of activities has important basic and therapeutic implications, since understanding what underlies this molecular decision could allow for manipulation of the triage process. The early observations of the degradative actions of chaperones did not include well-defined ubiquitin ligases (Lee *et al.*, 1996; Bercovich *et al.*, 1997; Fisher *et al.*, 1997; McClellan *et al.*, 2005). We, and others, have shown that a variety of misfolded full-length and truncated proteins undergo ubiquitination

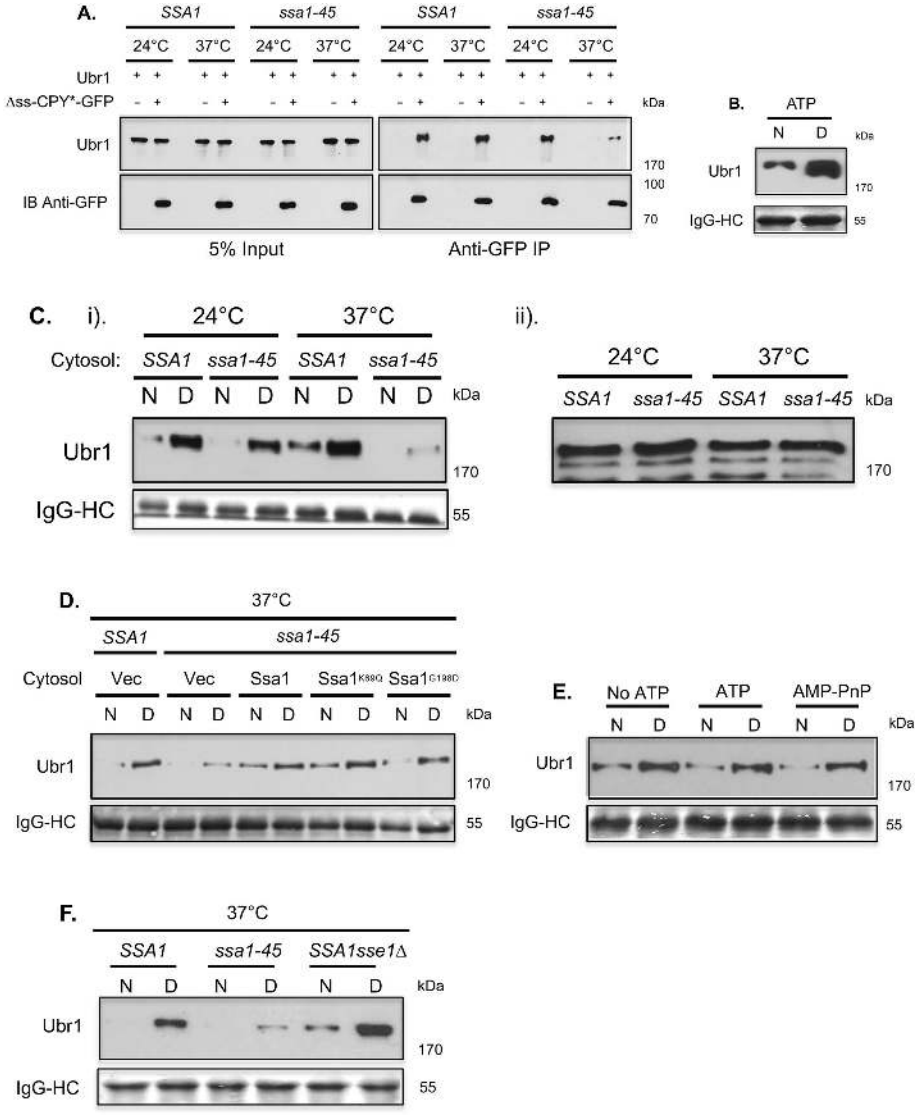

FIGURE 6: HSP70-mediated binding of Ubr1 to QC substrates. (A) Ubr1 interacted with Δss-CPY*-GFP in an HSP70-dependent manner. *Ssa1* or *ssa1-45* yeast expressing fl-Ubr1, along with empty vector or Δss-CPY*-GFP at 24°C, were harvested at 24°C or after 1 h at 37°C. Lysates were immunoprecipitated for Δss-CPY*-GFP and immunoblotted for Δss-CPY*-GFP (anti-GFP) or coprecipitated fl-Ubr1 (anti-FLAG). Five percentof the input was also immunoblotted to demonstrate equal loading. (B) Ubr1 associated with misfolded IgG in vitro. Native (N) or denatured (D) IgG beads were incubated with cytosol-containing fl-Ubr1 at 30°C for 40 min. Beads were then washed and subjected to immunoblotting to evaluate Ubr1 binding to the beads. (C) HSP70 was required for the interaction of Ubr1 with misfolded IgG. (i) Cytosols from Hsp70 strains in A were prepared and used to evaluate Ubr1 binding to native or denatured IgG beads. Cells were incubated at 24°C or 37°C for 1 h before preparation as indicated; binding assays were all performed at 30°C. (ii) The same cytosols were blotted for Ubr1 to confirm identical levels in all samples. Ssa1 levels were also identical in all cytosols (Supplemental Figure 7). (D) Ubr1 binding to misfolded IgG was independent of Ssa1 ATP binding and hydrolysis. Cytosols from WT or *ssa1-45* cells expressing the indicated Ssa1 mutants (or empty vector) were tested for ability to support fl-Ubr1 to misfolded substrate. One-hour preincubation of strains at 37°C is indicated. (E) HSP70-dependent Ubr1 binding to misfolded IgG was ATP-independent. Binding assays of fl-Ubr1 to immobilized IgG were performed as above in the absence or presence of indicated nucleotides. (F) Ubr1-binding to misfolded IgG was independent of Sse1. The *Ssa1ssa2Δssa3Δssa4Δ* strain used to observe the strong dependence of Ubr1 binding to misfolded IgG was made null for *SSE1* (*sse1Δ*) to examine Sse1 dependence of the HSP70-substrate-E3 interaction. Bottom panel demonstrates IgG load for each binding assay. Anti-GFP and anti-FLAG antibodies were used to detect Δss-CPY*-GFP and Ubr1, respectively. Anti-Ssa1 antibody was used to detect the levels of Ssa1. IgG-HC levels were assessed using India ink–stained blots.

by parallel actions of the Ubr1 and the San1 E3 ligases (Heck *et al.*, 2010; Nillegoda *et al.*, 2010; Prasad *et al.*, 2010). Both of these ligases show HSP70 dependence in the intact cell, providing an opportunity to explore how chaperone-mediated ubiquitination with multiple substrates of ligase defined in vivo QC pathways. We have found that the ATP hydrolytic cycle of HSP70 is intimately involved in the Ubr1-mediated ubiquitination of a variety of substrates. This parallelism suggests a hypothesis for HSP70-mediated triage that involves competing rates of chaperone-dependent folding versus chaperone-dependent ubiquitination (Figure 7).

In vivo, both HSP70 and HSP90 were required for the ubiquitin-mediated degradation of multiple substrates, including those that were degraded by both Ubr1 and San1 (Δss-CPY*-GFP and tGnd1-GFP) and the Ubr1-specific substrate stGnd1 (Figure 1). Moreover, HSP70 and HSP90 directly facilitated ubiquitination in vivo, with HSP70 showing the strongest requirement.

HSP70-mediated ATP hydrolysis was required for cytoplasmic substrate degradation and ubiquitination (Figure 2B). We observed that HSP70 mutants deficient in either nucleotide binding or hydrolysis exhibited defects in substrate degradation. Conversely, similar analysis of Sse1 mutants demonstrated that only the nucleotide exchange function of this cochaperone, and not ATP hydrolysis, was important for substrate degradation (Figure 2A). Mutant phenotypes were similarly strong for a variety of substrates, indicating a general role for HSP70-catalyzed hydrolysis and Sse1-mediated ATP exchange during degradation. Conversely, our study of the J-protein requirements gave a more complex picture, one that justifies the use of multiple substrates to unravel the role(s) of chaperones (Figure 2, C and D). Even when considering the partially redundant Ydj1/Hlj1 pair, distinct substrates of the Ubr1/San1 pathways were either strongly stabilized (tGnd1-GFP), partially stabilized (stGnd1), or destabilized (Δss-CPY*-GFP) (Figure 2C). Furthermore, for the Ubr1-only–dependent stGnd1, two separate classes of J-proteins were involved in degradation (Figure 2D). Significant stabilization was observed in strains deleted for the ribosome-associated Zuo1 and Jjj1 proteins as well as in the Ydj1 mutant. These data are consistent with the fact that there are a large number of yeast cochaperones, with overlapping functions among homologous types and between different classes (Kampinga and Craig, 2010; Cyr and Ramos, 2015; Dekker *et al.*, 2015).

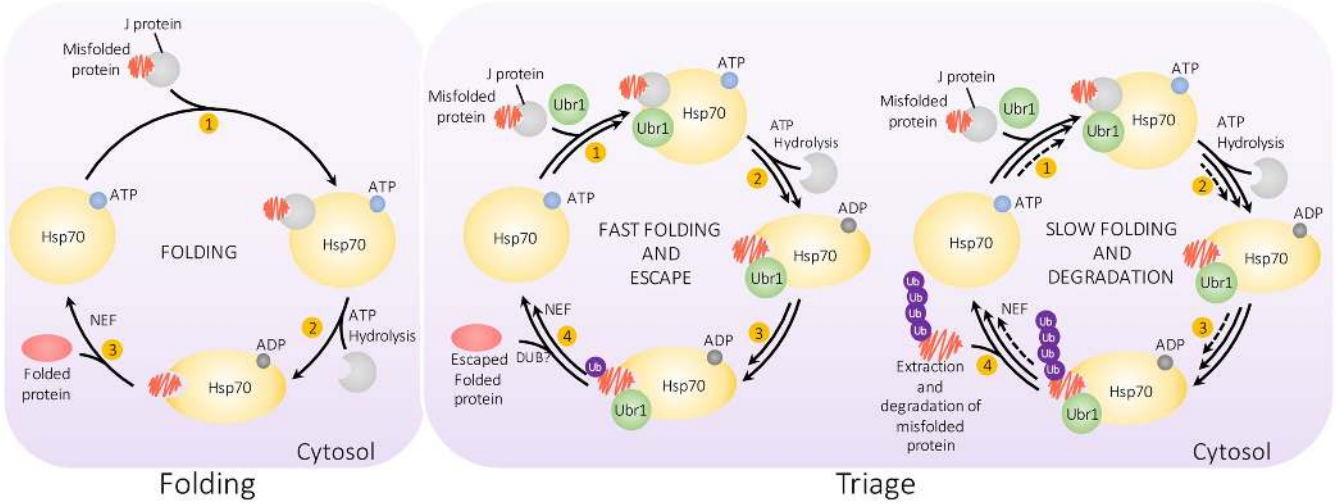

FIGURE 7: A "folding escape model" of Hsp70-mediated triage. As described in the text, the left panel shows Hsp70 acting alone to catalyze folding by ATP hydrolysis-dependent capture (steps 1 and 2) and release (step 3), in collaboration with Sse1 and J-proteins. The simultaneous occurrence of Ubr1-mediated ubiquitination of the folding substrate allows triage, manifest as a kinetic "race" between fast folding and escape (middle panel) or ubiquitination sufficient to trigger degradation before successful folding (step 4; right panel). Specific deubiquitinases may be present along with E3 ligases that control the degradation kinetics of substrate proteins, delaying/accelerating triage decisions.

In yeast, the J-proteins were involved in at least two aspects of QC, which include transport to the appropriate compartment (in the case of San1-dependent degradation) and direct involvement in Ubr1-mediated ubiquitination (Prasad *et al.*, 2018). The Sis1 J-protein, which is essential, was previously implicated in Δss-CPY*-GFP degradation (Park *et al.*, 2013; Figure 2E). Since a large component of Sis1-dependent degradation in our experiments is mediated by the nuclear San1 E3 ligase, and San1 may directly recognize structural abnormalities that limit its need for chaperones in multisubstrate detection (Rosenbaum *et al.*, 2011; Fredrickson *et al.*, 2013), we tested whether Sis1 promotes transport to the nucleus (Figure 2F). Modification of either the substrate or San1 to restrict its residence to the cytosol removed the Sis1 requirement for degradation (Figure 2F, i and ii). In contrast, Ubr1-dependent degradation was unaffected by reduction of Sis1 (Figure 2F). However, the Ubr1 exclusive substrate stGnd1 required J-proteins for degradation. Because we could not detect stGnd1 ubiquitination after substrate immunoprecipitation and ubiquitin immunoblotting, we evaluated stGnd1 ubiquitination with a substrate capture assay in which fl-stGnd1 was immunoprecipitated from Ubr1-deficient strains and then subjected to in vitro ubiquitination (Figure 3). stGnd1 ubiquitination was altered only by removal of Ubr1 (Figure 3A). In the in vitro assay, the Ydj1 component was preserved, since *ydj1-151hlj1*Δ cytosols attenuated ubiquitination (Figure 3D). Interestingly, *ydj1*Δ cells showed reduced ubiquitination of cytoplasmic VHL while having no effect on ubiquitination of nuclear VHL (Samant *et al.*, 2018). One model is that stGnd1 is first detected by ribosomal J-proteins cotranslationally and degraded in a Ubr1-dependent manner, while a portion that escapes the ribosome is subject to Ubr1-dependent degradation that is mediated by Ydj1. Since immunoprecipitated stGnd1 would consist of such escapees, this J-protein dependence appears to be preserved in the in vitro assay.

Our studies with J-proteins bring into relief a general difficulty in analyzing the role of chaperones in ubiquitination and QC. The chaperones and their cohorts are involved in a large number of distinct functions that include organelle-specific recognition, transport between compartments, alteration of aggregation state, solubilization, and possibly direct detection of substrates for E3 action and proteasomal destruction (Heck *et al.*, 2010; Hartl *et al.*, 2011; Saibil, 2013; Miller *et al.*, 2015; Rosenzweig *et al.*, 2019). Since misfolded proteins can undergo a variety of chaperone-dependent processes necessary for presentation of the substrate to its ligase in vivo, the actual chaperone dependence of Ubr1-dependent ubiquitination remained unclear. For instance, if a chaperone solubilizes a substrate before E3-mediated recognition, the Ubr1 pathway would still show strong chaperone-dependent ubiquitination despite its independence from E3 action. We obviated this concern by developing an assay that provides a more restricted presentation of misfolded substrates and that precluded effects of protein aggregation and chaperone-dependent solubilization. We employed IgG-agarose, in which IgG is chemically attached by sparse links to the beads, as well as disulfide-linked subunits attached to the proteins that are bead associated. Denaturation with heat or guanidinium does not disrupt the direct or disulfide attachments, allowing creation of a fully bead-bound QC substrate that can be presented to cytosols or other reagents to initiate the ubiquitination assay. This approach helped unravel direct from indirect effects of chaperones in CQC (Figure 5).

We believe that this bead-based, "solid state" approach has great utility in parsing the actions of chaperones; refinements of the assay will be valuable in a variety of studies. The studies herein rely on GdHCl denaturation, which was highly reproducible and consistent between experiments. We have also observed the same effects by using heat treatment of the IgG beads, although this method was harder to control. Clearly, GdHCl treatment is a strong treatment, resulting in wholesale misfolding of proteins (Hédoux *et al.*, 2010). It will be interesting to adapt the bead-bound assay to defined, misfolded mutants that are produced and then immobilized and to use this technique to understand chaperone triage in more physiological contexts, such as minimally misfolded proteins (Khosrow-Khavar *et al.*, 2012; Comyn *et al.*, 2016).

Immobilized IgG showed denaturation-specific ubiquitination of the bound IgG, such that ubiquitination of the untreated native

beads ("N" in assay lanes) was quite low (Figure 4). The in vivo ligase fidelity toward the bead-bound, denatured substrate was preserved; the Ubr1 component was strong, with San1 contributing in a more variable manner (Figures 4F and 5C). However, immobilization provided an approach that removes the contributions of substrate disaggregation or solubilization that could be provided by a chaperone in vivo. Nevertheless, the ubiquitination signal in the bead-bound assay was still HSP70-dependent. Cytosol prepared from the *ssa1-45* mutant could not support ubiquitination of the bound misfolded protein (Figure 5A). Using bead-bound IgG, we found that even when solubilization was not possible, the HSP70 ATPase cycle was required for Ubr1-mediated ubiquitination, as occurs in vivo (Figure 5B). The NEF Sse1 was also required for ubiquitination (Figure 5C). Furthermore, because of the accessibility of the bead-bound substrate, we could directly test the need for hydrolysis of the ATP γ-phosphate, which is required for chaperone action but not ubiquitin ligation (Figure 5E). Because the majority of activity in a typical assay is Ubr1-dependent, we assumed that the notable HSP70 requirement was due to its effects on this ligase. This was borne out by directly comparing degradation in WT, *sse1*Δ, and *ubr1*Δ strains all in a *san1*Δ background (Figure 5C); the strong Ubr1 component was completely Sse1-dependent and was not supported by AMP-PnP (Figure 5F). Conversely, an evaluation of a similar suite of *ubr1*Δ strains showed essentially no dependence on San1-supported ubiquitination of bead-bound misfolded IgG, consistent with San1's ability to detect substrates in a chaperone-independent manner (Supplemental Figure 8).

The biochemical accessibility of immobilized IgG allowed us to test the role of J-proteins with appropriate drugs. The inhibitory effect of the J-protein inhibitor MAL3-101, which abrogates J-protein stimulation of HSP70 (Fewell *et al.*, 2004), supported the expected J-protein requirement (Figure 5G). We posit that the J-proteins are involved in client recognition during HSP70-mediated triage and that J-protein–client interactions define client candidacy, and thus specificity, for this process. The large number of J-proteins and the overlapping specificity among some J-proteins create both a challenge in decoding specificity and a variety of opportunities for harnessing or modifying this process in the laboratory or in the clinic (Kampinga and Craig, 2010; Dekker *et al.*, 2015; Nillegoda *et al.*, 2015).

In striking contrast to the role of HSP70 in Ubr1-dependent ubiquitination of substrates both in vivo and in vitro, an HSP90 requirement was absent in the bead assay when either mutant cytosol or drugs (geldanamycin or RAD) were used. This was despite the fidelity of the bead-bound assay in recapitulating in vivo features (Figure 5H). Nevertheless, HSP90 was dispensable for either the Ubr1-dependent component or the smaller and variable San1-dependent component of ubiquitination. We posit that HSP90, while important in vivo, operates at a point distinct from recognition and processive ubiquitination of Ubr1-selective substrates. That being said, it will be important to discover what the role(s) of HSP90 are during QC ubiquitination in vivo, since a variety of substrates, including all we have tested and earlier substrates such as VHL require HSP90 for degradation in vivo (McClellan *et al.*, 2005).

We also capitalized on bead-bound QC to directly explore the role of HSP70 in Ubr1–substrate interactions. HSP70 is dispensable for the N-end rule function performed by Ubr1 (Lee *et al.*, 1996; Heck *et al.*, 2010), but appears to be strongly involved in QC. One reasonable model would be that HSP70 assists in detecting substrates and directing Ubr1 to these candidates for Ubr1-mediated modification. This is similar to the function of HSP70 proposed for CHIP, the U-box ligase implicated in chaperone-dependent QC in mammals (Qian *et al.*, 2006). If this were the case, we predict that the interaction of Ubr1 with QC substrates would depend on HSP70. HSP70 and Ubr1 have already been shown to interact (Summers *et al.*, 2013). We first tested this hypothesis with a traditional co-IP, using cell lysates expressing either the normal WT Ssa1 HSP70 or the Ssa1-45 *ts* mutant, similar to other studies examining substrate–Ubr1 interactions (Figure 6A; Stolz *et al.*, 2013; Summers *et al.*, 2013). Ubr1 associated with Δss-CPY*-GFP only when WT Ssa1 was expressed, or at the permissive temperature when the *ssa1-45* strain was employed. We next employed immobilized IgG, using the beads as an affinity platform to test interdependencies involved in the Ubr1–substrate interaction. Immobilized IgG binding gave a noticeably larger signal (perhaps due to the large unfolded surface area of the beads), allowing for direct comparisons between identical proteins in a folded or misfolded state and for direct addition of reagents. The interaction of Ubr1 with IgG in the assay was denaturation- and HSP70-dependent (Figure 6B). Inactivation of Ssa1 through the use of *ssa1-45* mutant cytosol caused a remarkable drop in Ubr1 binding to the denatured bead-bound IgG (usually about 30–50 fold), without any change in Ssa1 protein levels in the respective cytosols (Figure 6C). This dependence is similar to HSP70-assisted detection of Doa10 ERAD substrates and HSP70-dependent enhancement of CHIP binding to misfolded clients (Rosser *et al.*, 2007; Nakatsukasa *et al.*, 2008). As expected from the low dependence of San1 CQC ubiquitination on HSP70, the binding of San1 was unaffected by the presence or absence of functional HSP70 (Supplemental Figure 8).

The HSP70-dependent binding of Ubr1 to misfolded proteins makes sense if HSP70 brokers ligase specificity. In striking contrast to ubiquitination, the association of Ubr1 to misfolded substrates, despite being strongly dependent on HSP70, is ATP-independent (Figures 4F and 6E). Ubiquitination of misfolded immobilized IgG required external ATP, and its absence, or replacement with the AMP-PnP substrate, drastically curtailed ubiquitination (Figure 5E). Conversely, the absence of ATP or replacement with AMP-PnP had no effect on HSP70-dependent binding of Ubr1 to misfolded IgG (Figure 6E). Similarly, deletion of *Sse1* left Ubr1 binding to misfolded IgG fully intact (Figure 6F). Thus, substrate association with Ubr1 is strongly dependent on HSP70 but independent of the presence or the hydrolysis of ATP. This is quite different from the usual mechanism of action of this class of chaperones. Consistent with this result, the co-IP assay also showed HSP70-dependent binding of Δss-CPY*-GFP to Ubr1 in the absence of ATP or any added nucleotides (Figure 6A; Supplemental Figure 6).

From the above studies, we propose a model of Ubr1-mediated QC that provides a simple and perhaps general mechanism for the phenomenon of "protein triage" in which the same chaperone participates in both folding and degradation (Figure 7). The question surrounding triage has been, How does a chaperone perform these two apparently distinct actions, that is, how does it "know" which task is to be done? Our in vivo and in vitro data clearly show a "melding" of the folding and ubiquitination actions of HSP70 in the sense that the ATPase cycle, which is integral to the ability of this chaperone to refold proteins back to the native state (Figure 7, "Folding"), is also involved in the processive ubiquitination of misfolded substrates (Figure 7, "Triage"). Thus, the substrates being ubiquitinated also appear to be clients of the HSP70 capture-and-release process; that is, they are serving as HSP70 clients in the traditional sense while being simultaneously ubiquitinated by the E3. In circumstances where Ubr1 is available for binding to misfolded, HSP70-bound substrate (Figure 7, middle and right panels), both folding and ubiquitination occur during cycles of client capture and

release. If the ATP-dependent folding reaction is more efficient than the ATP-dependent ubiquitination reaction, then the folded client escapes before receiving sufficient ubiquitin additions to promote degradation (Figure 7, middle panel). In contrast, if ubiquitination is more efficient than the folding process, the ubiquitination of the slow-to-fold client will be sufficient to promote extraction and degradation before successful folding (Figure 7, right panel). In this view, triage is a "kinetic race" between two processes in which each employs the same cochaperones and the HSP70 ATPase cycle. Triage is thus a matter of the comparative efficiency of foldior ubiquitination, for those ligases that require the full chaperone cycle.

A similar "kinetic decision" model has been suggested for ER-associated degradation of lumenal glycoproteins (Molinari *et al.*, 2005; Soldà *et al.*, 2007). Here, misfolded proteins are captured and released by the lectin/chaperone calnexin in multiple cycles. If the client remains misfolded, it is glucosylated by UDP-glucose glycosyl transferase (UGGT), which is specific for misfolded substrates. However, during folding, the slower demannosylation of the triantennary glycosides can also occur, creating a modification that favors ERAD-mediated destruction. Thus, if the folding cycle is sufficiently fast, the substrate is spared from ERAD; if folding is sufficiently slow to allow competing demannosylation to occur, then destruction happens. So again, escape from degradation occurs by folding that is more efficient than a degradation-triggering modification. In the case of the "folding escape model" suggested in this study, the modification is ubiquitination itself, but the kinetic logic of the decision is similar. On the basis of our results, we speculate that when the folding sensor (HSP70) is missing, all the substrates meet a similar end, which is nonrecognition/escape from the degradation machinery.

The ATP-independence of Ubr1-CQC client binding suggests a simple ordering of the process. Any protein that binds to HSP70 will have Ubr1 placed in proximity. Then, if the ATPase cycle is activated by the collaboration of J-proteins and ATP/ADP exchange, the ubiquitination and folding reactions will start pari passu. Accordingly, protein triage by this model is more a matter of HSP70 restricting ubiquitination to those proteins that are chaperone clients, rather than the chaperone having different mechanisms to promote folding and degradation.

Because HSP70 has been implicated in a variety of degradative processes, including ERAD-C by Doa10 and CHIP-mediated destruction of misfolded proteins, it will be vital to examine the role of ATP cycling in these diverse yet thematically similar processes. Perhaps this folding rate versus ubiquitination rate model underlies various QC pathways. How does the ATP hydrolytic cycle promote ubiquitination? One possibility is that there are allosteric effects between the HSP70 and the E3 ligase that signal the folding cycle, and thus license the E3 to modify a participating client. Control of the degradation kinetics of Δss-CPY*-GFP by Ubp3 and Bre5 points to the involvement of deubiquitinases as well in the folding rate versus ubiquitination rate model (Jaeger and Ornelas *et al.*, 2018). Another is that the capture and release of substrates promotes E3 access to new modification sites or better catalytic access to growing chains. Whatever the mechanism, our model of a "kinetic race" provides several testable ideas and provides a mechanistic foothold onto this broadly observed use of chaperones in degradative QC (Figure 7).

MATERIALS AND METHODS

Yeast strains and plasmids

Saccharomyces cerevisiae strains used in this work are listed in Supplemental Table 1. All strains and plasmids were constructed with standard molecular biology techniques, as described previously (Gardner *et al.*, 1998; Gardner and Hampton, 1999). Yeast strains were cultured as described in minimal media with 2% dextrose and appropriate amino acid supplements, at 30°C unless otherwise indicated. The majority of strains used were in the BY4741 background, unless otherwise indicated in Supplemental Table 1. Null alleles with coding regions replaced were constructed in the BY4741 background by transforming yeast using the LiOAc method with a PCR product encoding the indicated selection marker and 50-base-pair flanks homologous to the gene to be disrupted or using knockout cassettes in the lab collection (Baudin *et al.*, 1993). Oligonucleotide sequences are available on request.

Degradation assays

Cycloheximide (CHX) chase degradation assays were performed as previously described (Gardner *et al.*, 1998). Briefly, yeast cells were grown to log phase (approximate $OD_{600} < 0.5$) and CHX was added to a final concentration of 50 µg/ml. At the indicated time points, cells were collected by centrifugation and lysed with 0.1 ml SUME (1% SDS, 8 M urea, 10 mM MOPS, pH 6.8, 10 mM EDTA) with protease inhibitors (PI) (260 µM ABESF, 142 µM TPCK, 100 µM leupeptin, 76 µM pepstatin) and 0.5 mm glass beads followed by vortexing for 2 min, followed by the addition of 100 µl 2× urea sample buffer (USB; 75 mM MOPS, pH 6.8, 4% SDS, 200 mM DTT, 0.2 mg/ml bromophenol blue, 8 M urea). The glass bead slurry was heated to 80°C for 5 min and then clarified by centrifugation before separation by SDS–PAGE and subsequent immunoblotting with appropriate antibodies. Degradation experiments involving temperature-sensitive mutants were carried out at 30°C and 37°C simultaneously. Preincubation of WT *SSA1* and *ssa1-45* mutant strains at 37°C was carried out for 30 min before the addition of CHX. Preincubation of WT *HSP82* and *hsp82*G170D mutant strains at 37°C was carried out for 1 h before CHX addition. Preincubation of WT *Ydj1* and *ydj1-151Δhlj1Δ* mutant strains at 37°C was carried out for 1 h before CHX addition. In the case of the Tet-OFF-Sis1 strain, cells were treated with 10 µM doxycycline for 20 h before CHX chase. For degradation assays involving inhibition of HSP82, cells were pretreated with 100 µM RAD and subjected to CHX chase for the indicated times.

Cytosol preparation

Cytosol for in vitro assays was prepared from the respective genetic backgrounds using an approach modified from in vitro ERAD assay developed in the laboratory (Garza *et al.*, 2009). Briefly, cells were grown in Yeast extract peptone dextrose media (YPD) to an OD_{600} of 0.8–1.0, and 100 ODs of cells was pelleted. The pellet was washed two times with H_2O and once with cold B88 (20 mM HEPES–KOH, pH 7.4, 150 mM KOAc, 250 mM sorbitol, and 5 mM $Mg(OAc)_2$) containing protease inhibitors (260 µM ABESF, 142 µM TPCK, 100 µM leupeptin, 76 µM pepstatin) and DTT and resuspended in 100 µl B88 with protease inhibitors (PI) and DTT for lysis by grinding in a mortar and pestle. The mortar and pestle were precooled with liquid nitrogen before the addition of the cells. The cells were added to the mortar containing 5 ml of liquid nitrogen. The frozen cells were ground by hand with the pestle. The cells were kept frozen during the process by the addition of liquid nitrogen as needed. The ground cells were then placed in a 2-ml tube on ice and allowed to thaw back to the liquid state. The resulting cytoplasm was clarified by centrifugation at 5000 × *g* at 4°C for 5 min. The supernatant was then transferred to a new tube and centrifuged again at 20,000 × *g* at 4°C for 15 min. A final ultracentrifugation was carried out at 100,000 × *g* at 4°C for 60 min. Protein concentration of cytosols was determined using a NanoDrop 2000

spectrophotometer. Cytosols were kept on ice until use or frozen in aliquots at –80°C.

In vitro ubiquitination assay

In vitro ubiquitination assays have been previously described (Heck *et al*., 2010). Bead-bound immunoprecipitated substrate was mixed with the isolated cytoplasm from the indicated genetic background in the following way: all cytoplasmic reactions took place in a final volume of 30 µl and were assembled on ice. Total protein (150 µg) from the respective cytoplasmic preparations was mixed with 7.5 mM ATP and 20 µl of FLAG beads bound to pre-IP substrate. The reactions were incubated in a 30°C water bath for 40 min with periodic agitation. The reaction was terminated by adding 500 µl of IP buffer (15 mM sodium phosphate, 150 mM NaCl, 10 mM EDTA, 2% Triton X-100, 0.1% SDS, 0.5% deoxycholate) with protease inhibitors and 5 mM *N*-ethylmaleimide. The FLAG beads were washed 3× with 1 ml IP wash (IPW) buffer (50 mM NaCl, 10 mM Tris, pH 7.5), aspirated to dryness, and heated in the presence of sample buffer to 100°C for 3 min before SDS–PAGE and immunoblotting.

Immunoprecipitation of substrate before in vitro ubiquitination experiments was conducted in the following manner: strains lacking Ubr1 but containing fl-stGnd1 were grown as described above for cytoplasmic preparation. Anti-FLAG M2 beads (20 µl) (A2220; Sigma Aldrich) were added per 4 ODs of cells and allowed to nutate overnight at 4°C. The beads were then pelleted at 2000 rpm for 30 s. Three washes with IP buffer were conducted before final resuspension in B88.

Preparation of immobilized substrate for bead-based ubiquitination was done using rabbit IgG-bound agarose beads (A2902; Sigma Aldrich). A typical experiment involved 400 µl of beads that were washed three times and then resuspended in 400 µl B88, as used in the in vitro ubiquitination procedure above. The bead suspension (200 µl) was then pelleted at 500 × *g* for 30 s, the solution was aspirated off, and the beads were resuspended in 1 ml of 6 M Gd-HCl and nutated in a cold room for 20 min. One milliliter of B88 was added to the remaining 200 µl bead suspension. Thereafter, the beads were pelleted at 500 × *g* for 30 s, and Gd-HCl was aspirated. The beads were washed four times with B88 and then resuspended in 200 µl B88. Twenty microliters of resuspended beads was used per reaction. After the completion of the reaction, the cytosol was aspirated and 2× USB was added.

In experiments that involved treatment of the cytosol with small molecules, 150 µg of cytosol was incubated with either 2.5% (vol/vol) dimethyl sulfoxide (DMSO) or 50 µM MAL2-11B or MAL3-101 or 100 µM RAD.

In vivo ubiquitination assay

The in vivo ubiquitination of substrates was evaluated by IP followed by ubiquitin immunoblotting as described (Heck *et al*., 2010). After being vortexed in the presence of glass beads and SUME at 4°C for 10 min, 1 ml of IP buffer with protease inhibitors and *N*-ethylmaleimide was added. The lysate was clarified by centrifugation at 15,000 rpm for 5 min. The supernatant was transferred to a new tube, and either polyclonal anti-GFP, anti-HA (Covance), or monoclonal anti-FLAG M2 beads (Sigma-Aldrich) was added, depending on the substrate. The lysates were nutated overnight at 4°C. In the case of anti-GFP and anti-HA pull downs, Protein A–Sepharose beads (100 µl) were then added and allowed to nutate for an additional 2 h at 4°C. The beads were then spun down at 2000 rpm for 30 s, and washed three times with IP wash buffer (50 mM NaCl, 10 mM Tris, pH 7.5), and aspirated to dryness before the addition of 50 µl of electrophoretic sample buffer.

For looking at in vivo ubiquitination of Δss-CPY*-GFP and tGND1-GFP, in the context of inhibition of HSP82, cells were pretreated with 100 µM RAD for 1 h and subjected to IP as indicated previously.

Native co-IP protocol

The native co-IP assay was performed as described previously (Vashistha *et al*., 2016). Isogenic yeast strains with or without substrate were lysed by bead beating in co-IP buffer (20 mM HEPES, pH 7, 150 mM NaCl, 1% CHAPS). The lysates were harvested, and the beads were washed with 1 ml of Tween IP buffer (500 mM NaCl, 50 mM HEPES, pH 7.5, 100 mM EDTA, 1.5% Tween-20). The pooled supernatant was then clarified to remove unbroken cells and debris. The clarified supernatant was then incubated with 15 µl of either anti-GFP or anti-FLAG antibody overnight at 4°C followed by 2 h with Protein A–Sepharose beads. The beads were then washed with the Tween-20 IP buffer and incubated with 50 µl of 2× USB for 10 min at 70°C. The samples were then analyzed on 8% SDS–PAGE.

Antibodies and immunoblotting

Immunoblotting was carried out subsequent to electrophoresis and transfer to nitrocellulose membrane using the following antibodies. The blocking solution for all antibodies was 5% milk in TBST (10 mM Tris, pH 8.0, 150 mM NaCl, 0.5% [vol/vol] Tween-20), apart from anti-ubiquitin, for which 20% heat-inactivated calf-serum in TBSHT (TBSHT with 0.5% [vol/vol] Tween-20). To detect ubiquitin, nitrocellulose membranes were also microwaved for 3 min while submerged in water. Mouse anti-HA antibody was obtained from Covance and used at a dilution of 1:10,000. Monoclonal anti-GFP antibody was obtained from Clontech (Living Colors) and was used at a dilution of 1:10,000. Monoclonal anti-ubiquitin antibody was procured from the Fred Hutchinson Cancer Research Centre, Seattle, WA, and used at a dilution of 1:10,000. Mouse anti–HSV-tag antibody was from Novagen and used at a 1:10,000 dilution. Monoclonal anti-FLAG M2 antibody was obtained from Sigma-Aldrich and used at a dilution of 1:2500. Rabbit anti-Ssa1 antibodies were used at a dilution of 1:2500.

ACKNOWLEDGMENTS

We thank Elizabeth Craig (University of Wisconsin, Madison), Judith Frydman (Stanford University), Richard Gardner (University of Washington, Seattle), Kevin Morano (University of Texas, Houston), Davis Ng (Tamasek Life Sciences Institute, Singapore), F. Ulrich Hartl (Max Planck Institute of Biochemistry, Germany), Alex Varshavsky (California Institute of Technology), and the late Susan Lindquist (Whitehead Institute, MIT) for strains and/or plasmids. We thank all members of the Hampton group for many fruitful discussions and vigilant attention to intellectual quality control. R.Y.H. further thanks M. Highsmith-Hampton for "Bee plus" work in all relevant fields. A. S. thanks Dimple Notani and Anaya Singh for the unwavering love and support. This research was supported by National Institutes of Health grants GM092748 (R.Y.H.), GM075061, GM131732 and DK079307 (J.L.B.), and GM067082 (P. W.).

REFERENCES

Amm I, Wolf DH (2016). Molecular mass as a determinant for nuclear San1-dependent targeting of misfolded cytosolic proteins to proteasomal degradation. FEBS Lett 590, 1765–1775.

Aron R, Higurashi T, Sahi C, Craig EA (2007). J-protein co-chaperone Sis1 required for generation of [*RNQ*+] seeds necessary for prion propagation. EMBO J 26, 3794–3803.

Balch WE, Morimoto RI, Dillin A, Kelly JW (2008). Adapting proteostasis for disease intervention. Science 319, 916–919.

Baudin A, Ozier-Kalogeropoulos O, Denouel A, Lacroute F, Cullin C (1993). A simple and efficient method for direct gene deletion in Saccharomyces cerevisiae. Nucleic Acids Res 21, 3329–3330.
Bercovich B, Stancovski I, Mayer A, Blumenfeld N, Laszlo A, Schwartz AL, Ciechanover A (1997). Ubiquitin-dependent degradation of certain protein substrates in vitro requires the molecular chaperone Hsc70. J Biol Chem 272, 9002–9010.
Brandman O, Hegde RS (2016). Ribosome-associated protein quality control. Nat Struct Mol Biol 23, 7–15.
Chen B, Retzlaff M, Roos T, Frydman J (2011). Cellular strategies of protein quality control. Cold Spring Harb Perspect Biol 3, a004374.
Comyn SA, Young BP, Loewen CJ, Mayor T (2016). Prefoldin promotes proteasomal degradation of cytosolic proteins with missense mutations by maintaining substrate solubility. PLoS Genet 12, e1006184.
Cyr DM, Ramos CH (2015). Specification of Hsp70 function by type and type II Hsp40. In: The Networking of Chaperones and Co-chaperones, Vol. 78, Subcellular Biochemistry, Elsevier, 91–102.
Dekker SL, Kampinga HH, Bergink S (2015). DNAJs: more than substrate delivery to HSPA. Front Mol Biosci 2, 35.
Doyle SM, Genest O, Wickner S (2013). Protein rescue from aggregates by powerful molecular chaperone machines. Nat Rev Mol Cell Biol 14, 617–629.
Dragovic Z, Broadley SA, Shomura Y, Bracher A, Hartl FU (2006). Molecular chaperones of the Hsp110 family act as nucleotide exchange factors of Hsp70s. EMBO J 25, 2519–2528.
Enam C, Geffen Y, Ravid T, Gardner RG (2018). Protein quality control degradation in the nucleus. Annu Rev Biochem 87, 725–749.
Fewell SW, Smith CM, Lyon MA, Dumitrescu TP, Wipf P, Day BW, Brodsky JL (2004). Small molecule modulators of endogenous and co-chaperone-stimulated Hsp70 ATPase activity. J Biol Chem 279, 51131–51140.
Fisher EA, Zhou M, Mitchell DM, Wu X, Omura S, Wang H, Goldberg AL, Ginsberg HN (1997). The degradation of apolipoprotein B100 is mediated by the ubiquitin-proteasorne pathway and involves heat shock protein 70. J Biol Chem 272, 20427–20434.
Fredrickson EK, Gallagher PS, Candadai SVC, Gardner RG (2013). Substrate recognition in nuclear protein quality control degradation is governed by exposed hydrophobicity that correlates with aggregation and insolubility. J Biol Chem 288, 6130–6139.
Gallagher PS, Clowes Candadai SV, Gardner RG (2014). The requirement for Cdc48/p97 in nuclear protein quality control degradation depends on the substrate and correlates with substrate insolubility. J Cell Sci 127, 1980–1991.
Gardner R, Cronin S, Leader B, Rine J, Hampton R, Leder B (1998). Sequence determinants for regulated degradation of yeast 3-hydroxy-3-methylglutaryl-CoA reductase, an integral endoplasmic reticulum membrane protein [correction published in Mol Biol Cell (1999), 10]. Mol Biol Cell 9, 2611–2626.
Gardner RG, Hampton RY (1999). A highly conserved signal controls degradation of 3-hydroxy-3- methylglutaryl-coenzyme a (HMG-CoA) reductase in eukaryotes. J Biol Chem 274, 31671–31678.
Gardner RG, Nelson ZW, Gottschling DE (2005). Degradation-mediated protein quality control in the nucleus. Cell 120, 803–815.
Garza RM, Sato BK, Hampton RY (2009). In vitro analysis of Hrd1p-mediated retrotranslocation of its multispanning membrane substrate 3-hydroxy-3-methylglutaryl (HMG)-CoA reductase. J Biol Chem 284, 14710–14722.
Goeckeler JL, Petruso AP, Aguirre J, Clement CC, Chiosis G, Brodsky JL (2008). The yeast Hsp110, Sse1p, exhibits high-affinity peptide binding. FEBS Lett 582, 2393–2396.
Gowda NKC, Kandasamy G, Froehlich MS, Jürgen Dohmen R, Andréasson C (2013). Hsp70 nucleotide exchange factor Fes1 is essential for ubiquitin-dependent degradation of misfolded cytosolic proteins. Proc Natl Acad Sci USA 110, 5975–5980.
Guerriero CJ, Brodsky JL (2012). The delicate balance between secreted protein folding and endoplasmic reticulum-associated degradation in human physiology. Physiol Rev 92, 537–576.
Guerriero CJ, Weiberth KF, Brodsky JL (2013). Hsp70 targets a cytoplasmic quality control substrate to the San1p ubiquitin ligase. J Biol Chem 288, 18506–18520.
Hampton RY, Dargemont C (2017). New developments for protein quality control. Science 357, 450–451.
Hampton RY, Sommer T (2012). Finding the will and the way of ERAD substrate retrotranslocation. Curr Opin Cell Biol 24, 460–466.
Hartl FU, Bracher A, Hayer-Hartl M (2011). Molecular chaperones in protein folding and proteostasis. Nature 475, 324–332.
Heck JW (2010). Discovery of ubiquitin ligases involved in cytoplasmic quality control. Doctoral thesis, UC San Diego. Available at: https://escholarship.org/uc/item/4r95t5c0 (accessed 9 October 2020).
Heck JW, Cheung SK, Hampton RY (2010). Cytoplasmic protein quality control degradation mediated by parallel actions of the E3 ubiquitin ligases Ubr1 and San1. Proc Natl Acad Sci USA 107, 1106–1111.
Hédoux A, Krenzlin S, Paccou L, Guinet Y, Flament MP, Siepmann J (2010). Influence of urea and guanidine hydrochloride on lysozyme stability and thermal denaturation; a correlation between activity, protein dynamics and conformational changes. Phys Chem Chem Phys 12, 13189–13196.
Hipp M, Kasturi P, Hartl FU (2019). The proteostasis network and its decline in ageing. Nat Rev Mol Cell Biol 20, 421–435.
Huang P, Gautschi M, Walter W, Rospert S, Craig EA (2005). The Hsp70 Ssz1 modulates the function of the ribosome-associated J-protein Zuol. Nat Struct Mol Biol 12, 497–504.
Huryn DM, Brodsky JL, Brummond KM, Chambers PG, Eyer B, Ireland AW, Kawasumi M, LaPorte MG, Lloyd K, Manteau B, *et al*. (2011). Chemical methodology as a source of small-molecule checkpoint inhibitors and heat shock protein 70 (Hsp70) modulators. Proc Natl Acad Sci USA 108, 6757–6762.
Jaeger PA, Ornelas L, McElfresh C, Wong LR, Hampton RY, Ideker T (2018). Systematic gene-to-phenotype arrays: a high-throughput technique for molecular phenotyping. Mol Cell 69, 321–333.e3.
Joazeiro CAP (2019). Mechanisms and functions of ribosome-associated protein quality control. Nat Rev Mol Cell Biol 20, 368–383.
Jones RD, Enam C, Ibarra R, Borror HR, Mostoller KE, Fredrickson EK, Lin J, Chuang E, March Z, Shorter J, *et al*. (2020). The extent of Ssa1/Ssa2 Hsp70 chaperone involvement in nuclear protein quality control degradation varies with the substrate. Mol Biol Cell 31, 221–233.
Kampinga HH, Craig EA (2010). The HSP70 chaperone machinery: J proteins as drivers of functional specificity. Nat Rev Mol Cell Biol 11, 579–592.
Kandasamy G, Andreasson C (2018). Hsp70–Hsp110 chaperones deliver ubiquitin-dependent and -independent substrates to the 26S proteasome for proteolysis in yeast. J Cell Sci 131, jcs210948.
Khosrow-Khavar F, Fang N, Ng A, Winget J, Comyn S, Mayor T (2012). The yeast Ubr1 ubiquitin ligase participates in a prominent pathway that targets cytosolic thermosensitive mutants for degradation. G3 2, 619–628.
Klaips C, Jayaraj GG, Hartl FU (2018). Pathways of cellular proteostasis in aging and disease. J Cell Biol 217, 51–63.
Kriegenburg F, Jakopec V, Poulsen EG, Nielsen SV, Roguev A, Krogan N, Gordon C, Fleig U, Hartmann-Petersen R (2014). A chaperone-assisted degradation pathway targets kinetochore proteins to ensure genome stability. PLoS Genet 10, e1004140.
Lee DH, Sherman MY, Goldberg AL (1996). Involvement of the molecular chaperone Ydj1 in the ubiquitin-dependent degradation of short-lived and abnormal proteins in Saccharomyces cerevisiae. Mol Cell Biol 16, 4773–4781.
Lee MJ, Lee BH, Hanna J, King RW, Finley D (2011). Trimming of ubiquitin chains by proteasome-associated deubiquitinating enzymes. Mol Cell Proteomics 10, R110.003871.
Liu XD, Morano KA, Thiele DJ (1999). The yeast Hsp110 family member, Sse1, is an Hsp90 cochaperone. J Biol Chem 274, 26654–26660.
Lykke-Andersen J, Bennett EJ (2014). Protecting the proteome: eukaryotic cotranslational quality control pathways. J Cell Biol 204, 467–476.
McClellan AJ, Brodsky JL (2000). Mutation of the ATP-binding pocket of SSA1 indicates that a functional interaction between Ssa1p and Ydj1p is required for post-translational translocation into the yeast endoplasmic reticulum. Genetics 156, 501–512.
McClellan AJ, Scott MD, Frydman J (2005). Folding and quality control of the VHL tumor suppressor proceed through distinct chaperone pathways. Cell 121, 739–748.
Metzger MB, Pruneda JN, Klevit RE, Weissman AM (2014). RING-type E3 ligases: master manipulators of E2 ubiquitin-conjugating enzymes and ubiquitination. Biochim Biophys Acta 1843, 47–60.
Metzger MB, Scales JL, Dunklebarger MF, Loncarek J, Weissman AM (2020). A protein quality control pathway at the mitochondrial outer membrane. eLife 9, e51065.
Miller SBM, Mogk A, Bukau B (2015). Spatially organized aggregation of misfolded proteins as cellular stress defense strategy. J Mol Biol 427, 1564–1574.
Molinari M, Galli C, Vanoni O, Arnold SM, Kaufman RJ (2005). Persistent glycoprotein misfolding activates the glucosidase II/UGT1-driven calnexin cycle to delay aggregation and loss of folding competence. Mol Cell 20, 503–512.

Nakatsukasa K, Huyer G, Michaelis S, Brodsky JL (2008). Dissecting the ER-associated degradation of a misfolded polytopic membrane protein. Cell 132, 101–112.
Nathan DF, Lindquist S (1995). Mutational analysis of Hsp90 function: interactions with a steroid receptor and a protein kinase. Mol Cell Biol 15, 3917–3925.
Needham PG, Patel HJ, Chiosis G, Thibodeau PH, Brodsky JL (2015). Mutations in the yeast Hsp70, Ssa1, at P417 alter ATP cycling, inter-domain coupling, and specific chaperone functions. J Mol Biol 427, 2948–2965.
Nillegoda NB, Kirstein J, Szlachcic A, Berynskyy M, Stank A, Stengel F, Arnsburg K, Gao X, Scior A, Aebersold R, *et al.* (2015). Crucial HSP70 co-chaperone complex unlocks metazoan protein disaggregation. Nature 524, 247–251.
Nillegoda NB, Theodoraki MA, Mandal AK, Mayo KJ, Ren HY, Sultana R, Wu K, Johnson J, Cyr DM, Caplan AJ (2010). Ubr1 and Ubr2 function in a quality control pathway for degradation of unfolded cytosolic proteins. Mol Biol Cell 21, 2102–2116.
Nishikawa SI, Fewell SW, Kato Y, Brodsky JL, Endo T (2001). Molecular chaperones in the yeast endoplasmic reticulum maintain the solubility of proteins for retrotranslocation and degradation. J Cell Biol 153, 1061–1070.
Park SH, Bolender N, Eisele F, Kostova Z, Takeuchi J, Coffino P, Wolf DH (2007). The cytoplasmic Hsp70 chaperone machinery subjects misfolded and endoplasmic reticulum import-incompetent proteins to degradation via the ubiquitin-proteasome system. Mol Biol Cell 18, 153–165.
Park SH, Kukushkin Y, Gupta R, Chen T, Konagai A, Hipp MS, Hayer-Hartl M, Hartl FU (2013). PolyQ proteins interfere with nuclear degradation of cytosolic proteins by sequestering the Sis1p chaperone. Cell 154, 134–145.
Park SK, Hong JY, Arslan F, Kanneganti V, Patel B, Tietsort A, Tank EMH, Li X, Barmada SJ, Liebman SW (2017). Overexpression of the essential Sis1 chaperone reduces TDP-43 effects on toxicity and proteolysis. PLoS Genet 13, e1006805.
Phillips BP, Gomez-Navarro N, Miller EA (2020). Protein quality control in the endoplasmic reticulum. Curr Opin Cell Biol 65, 96–102.
Pohl C, Dikic I (2019). Cellular quality control by the ubiquitin-proteasome system and autophagy. Science 366, 818–822.
Prasad R, Kawaguchi S, Ng DTW (2010). A nucleus-based quality control mechanism for cytosolic proteins. Mol Biol Cell 21, 2117–2127.
Prasad R, Xu C, Ng DTW (2018). Hsp40/70/110 chaperones adapt nuclear protein quality control to serve cytosolic clients. J Cell Biol 217, 2019–2032.
Pruneda JN, Littlefield PJ, Soss SE, Nordquist KA, Chazin WJ, Brzovic PS, Klevit RE (2012). Structure of an E3:E2~;Ub complex reveals an allosteric mechanism shared among RING/U-box ligases. Mol Cell 47, 933–942.
Qian SB, McDonough H, Boellmann F, Cyr DM, Patterson C (2006). CHIP-mediated stress recovery by sequential ubiquitination of substrates and Hsp70. Nature 440, 551–555.
Raviol H, Sadlish H, Rodriguez F, Mayer MP, Bukau B (2006). Chaperone network in the yeast cytosol: Hsp110 is revealed as an Hsp70 nucleotide exchange factor. EMBO J 25, 2510–2518.
Rosenbaum JC, Fredrickson EK, Oeser ML, Garrett-Engele CM, Locke MN, Richardson LA, Nelson ZW, Hetrick ED, Milac TI, Gottschling DE, *et al.* (2011). Disorder targets misorder in nuclear quality control degradation: a disordered ubiquitin ligase directly recognizes its misfolded substrates. Mol Cell 41, 93–106.
Rosenzweig R, Nillegoda NB, Mayer MP, Bukau B (2019). The Hsp70 chaperone network. Nat Rev Mol Cell Biol 20, 665–680.
Rosser MFN, Washburn E, Muchowski PJ, Patterson C, Cyr DM (2007). Chaperone functions of the E3 ubiquitin ligase CHIP. J Biol Chem 282, 22267–22277.
Sahi C, Craig EA (2007). Network of general and specialty J protein chaperones of the yeast cytosol. Proc Natl Acad Sci USA 104, 7163–7168.
Saibil H (2013). Chaperone machines for protein folding, unfolding and disaggregation. Nat Rev Mol Cell Biol 14, 630–642.
Samant RS, Livingston CM, Sontag EM, Frydman J (2018). Distinct proteostasis circuits cooperate in nuclear and cytoplasmic protein quality control. Nature 563, 407–411.
Sato BK, Schulz D, Do PH, Hampton RY (2009). Misfolded membrane proteins are specifically recognized by the transmembrane domain of the Hrd1p ubiquitin ligase. Mol Cell 34, 212–222.
Shaner L, Sousa R, Morano KA (2006). Characterization of Hsp70 binding and nucleotide exchange by the yeast Hsp110 chaperone Sse1. Biochemistry 45, 15075–15084.
Shaner L, Wegele H, Buchner J, Morano KA (2005). The yeast Hsp110 Sse1 functionally interacts with the Hsp70 chaperones Ssa and Ssb. J Biol Chem 280, 41262–41269.
Soldà T, Galli C, Kaufman RJ, Molinari M (2007). Substrate-specific requirements for UGT1-dependent release from calnexin. Mol Cell 27, 238–249.
Stolz A, Besser S, Hottmann H, Wolf DH (2013). Previously unknown role for the ubiquitin ligase Ubr1 in endoplasmic reticulum-associated protein degradation. Proc Natl Acad Sci USA 110, 15271–15276.
Summers DW, Wolfe KJ, Ren HY, Cyr DM (2013). The type II Hsp40 Sis1 cooperates with Hsp70 and the E3 ligase Ubr1 to promote degradation of terminally misfolded cytosolic protein. PLoS One 8, e52099.
Sun Z, Diaz Z, Fang X, Hart MP, Chesi A, Shorter J, Gitler AD (2011). Molecular determinants and genetic modifiers of aggregation and toxicity for the ALS disease protein FUS/TLS. PLoS Biol 9, e1000614.
Terrab L, Wipf P (2020). Hsp70 and the unfolded protein response as a challenging drug target and an inspiration for probe molecule development. ACS Med Chem Lett 11, 232–236.
Theodoraki MA, Nillegoda NB, Saini J, Caplan AJ (2012). A network of ubiquitin ligases is important for the dynamics of misfolded protein aggregates in yeast. J Biol Chem 287, 23911–23922.
Vashistha N, Neal SE, Singh A, Carroll SM, Hampton RY (2016). Direct and essential function for Hrd3 in ER-associated degradation. Proc Natl Acad Sci USA 113, 5934–5939.
Verma R, Oania RS, Kolawa NJ, Deshaies RJ (2013). Cdc48/p97 promotes degradation of aberrant nascent polypeptides bound to the ribosome. eLife 2, e00308.
Walden H, Podgorski MS, Schulman BA (2003). Insights into the ubiquitin transfer cascade from the structure of the activating enzyme for NEDD8. Nature 422, 330–334.
Walters RW, Muhlrad D, Garcia J, Parker R (2015). Differential effects of Ydj1 and Sis1 on Hsp70-mediated clearance of stress granules in Saccharomyces cerevisiae. RNA 21, 1660–1671.
Wangeline M, Vashistha N, Hampton RY (2017). Proteostatic tactics in the strategy of sterol regulation. Annu Rev Cell Dev Biol 33, 467–489.
Wisén S, Bertelsen EB, Thompson AD, Patury S, Ung P, Chang L, Evans CG, Walter GM, Wipf P, Carlson HA, *et al.* (2010). Binding of a small molecule at a protein-protein interface regulates the chaperone activity of Hsp70-Hsp40. ACS Chem Biol 5, 611–622.
Wu X, Siggel M, Ovchinnikov S, Mi W, Svetlov V, Nudler E, Liao M, Hummer G, Rapoport TA (2020). Structural basis of ER-associated protein degradation mediated by the Hrd1 ubiquitin ligase complex. Science 368, eaaz2449.
Youker RT, Walsh P, Beilharz T, Lithgow T, Brodsky JL (2004). Distinct roles for the Hsp40 and Hsp90 molecular chaperones during cystic fibrosis transmembrane conductance regulator degradation in yeast. Mol Biol Cell 15, 4787–4797.
Zattas D, Hochstrasser M (2015). Ubiquitin-dependent protein degradation at the yeast endoplasmic reticulum and nuclear envelope. Crit Rev Biochem Mol Biol 50, 1–17.